IEEE Access
Multidisciplinary | Rapid Review | Open Access Journal

Received November 27, 2020, accepted December 20, 2020, date of publication December 29, 2020,
date of current version January 13, 2021.

Digital Object Identifier 10.1109/ACCESS.2020.3048049

A Survey of Free Space Optics (FSO) Communication Systems, Links, and Networks

SAMIR AHMED AL-GAILANI[1,5], (Member, IEEE), MOHD FADZLI MOHD SALLEH[1], (Member, IEEE), ALI AHMED SALEM[2], (Member, IEEE), REDHWAN QASEM SHADDAD[3], USMAN ULLAH SHEIKH[4], (Member, IEEE), NASIR AHMED ALGEELANI[5], AND TARIK A. ALMOHAMAD[6], (Student Member, IEEE)

[1]School of Electrical and Electronic Engineering, Universiti Sains Malaysia, Nibong Tebal 14300, Malaysia
[2]Faculty of Electrical and Electronic Engineering, Universiti Tun Hussein Onn Malaysia, Batu Pahat 86400, Malaysia
[3]Faculty of Engineering and Information Technology, Taiz University, Taiz, Yemen
[4]Faculty of Engineering, School of Electrical Engineering, Universiti Teknologi Malaysia, Johor Bahru 81310, Malaysia
[5]Department of Electrical and Electronics Engineering, Faculty of Engineering, Al-Madinah International University, Kuala Lumpur 57100, Malaysia
[6]Electrical-Electronics Engineering Department, Faculty of Engineering, Karabük University, 78050 Karabük, Turkey

Corresponding authors: Mohd Fadzli Mohd Salleh (fadzlisalleh@usm.my) and Ali Ahmed Salem (en.alisalem@gmail.com)

This work was supported in part by the University of Science Malaysia under Grant 304/PELECT/6315344.

ABSTRACT The next generation (NG) optical technologies will unveil certain unique features, namely ultra-high data rate, broadband multiple services, scalable bandwidth, and flexible communications for manifold end-users. Among the optical technologies, free space optical (FSO) technology is a key element to achieve free space data transmission according to the requirements of the future technologies, which is due to its cost effective, easy deployment, high bandwidth enabler, and high secured. In this article, we give the overview of the recent progress on FSO technology and the factors that will lead the technology towards ubiquitous application. As part of the review, we provided fundamental concepts across all types of FSO system, including system architecture comprising of single beam and multiple beams. The review is further expanded into the investigation of rain and haze effects toward FSO signal propagation. The final objective that we cover is the scalability of an FSO network via the implementations of hybrid multi-beam FSO system with wavelength division multiplexing (WDM) technology.

INDEX TERMS FSO, rain attenuation, haze attenuation, DWDM multiplexing, and scalability.

I. INTRODUCTION

The FSO communication system is one of the prominent wireless communication systems, which witnessed a massively increasing interest and vast development in the last decade [1]. Some of other terminologies used for FSO technology are Wireless Optical Communication (WOC) [2], Fiber-less [3], and Laser Communication (Lasercom) [2]. In terms of broadband communication service, FSO is regarded as a suitable candidate to offer this service to the end users, with specific demand of point to point connection, under clear atmospheric environment in between transmitter and receiver. In comparison to fiber optic transmission, FSO technologies are principally the same.

The difference is that FSO output is collimated and transmitted through atmosphere, while fiber optic transmission will have its output transmitted via optical fiber [4]. FSO provides a unique alternative compared to the current technologies, which can meet the exponentially growing demand for bandwidth.

Most importantly, optical fiber cable can be replaced with FSO systems in scenarios where either cables cannot be laid or requires high capital expenditure (CAPEX) [5], [6]. Some of the key advantages of FSO technology are large bandwidth, immune to electromagnetic interference, no spectrum licensing, and higher data rate. However, an FSO transmission is prone to the non-ideal conditions arising from unstable

The associate editor coordinating the review of this manuscript and approving it for publication was Nianqiang Li.

weather conditions. In other word, single beam FSO system is susceptible to weather conditions whereby turbulence, rain, fog, haze and dust [7] introduces attenuation to the light source or even block the propagation. Hence, FSO system should be thoroughly investigated relative to weather conditions, to ensure that the received power is sufficient at the receiver for processing. An alternative solution to minimize these effects is the use of multiple beam FSO system [7] jointly with wavelength division multiplexing (WDM) technique for efficient and scalable network [8]. Many studies were carried out under different environmental conditions and its relative impact to the performance of FSO system [9]. To the best of our knowledge some of the studies have been investigated the FSO transmission conditions in Malaysia, therefore this article will review the properties of the FSO systems and link performance under tropical condition.

This article is organized as the followings, II covers the FSO system in general followed by thorough discussion of various components along the link. III is dedicated to report on the atmospheric conditions that affect the FSO communication, while IV unveils the design of Hybrid WDM/Multi-beam FSO Network. Finally, the conclusions are drawn in V.

II. FSO COMMUNICATION SYSTEM

The transmission of data from FSO transmitter to FSO receiver is performed by using a modulated narrow optical laser beam which is used to carry the digital data from transmitter to receiver via free space atmosphere and finally processed at the receiving station [10]. Line of sight simply means that the transmitter and the receiver at both networking locations can see each other. Because IR beams propagate and expand in a linear fashion, the line of sight criteria is less strict when compared to microwave systems that require an additional path clearance to account for the extension of Fresnel zones [11]. In modelling any free space channel, the Fresnel zone is taken into account [12]. Fig. 1 shows some examples of the correct and incorrect installation of the wireless antennas on the towers regarding Fresnel zone. The Fresnel Zone is the area around the visual line-of-sight that radio waves spread out into, after they leave the antenna. Fresnel Zones are described as the circular cross sections between two wireless devices that must be clear of any objects or obstacles to avoid any degradation in signal quality [13].

As it is well-known that the size of the Fresnel Zone is proportional to the wavelength of the signal, it is found that the larger the wavelength the bigger the Fresnel Zone is (the area that must be clear). To avoid any complex calculations, the size of the 5 GHz Fresnel Zone is taken as about half that of 2.4GHz meaning that less free space is required between the two points [14].

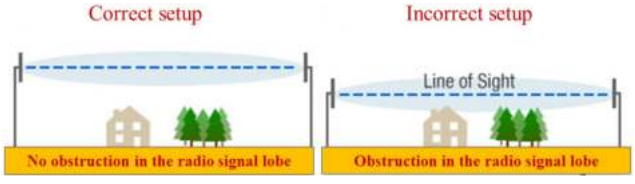

FIGURE 1. Examples of the correct and incorrect installation of the wireless antennas on the towers.

A. FSO TRANSCEIVER MODULE

The FSO communication system in static placement comprises of three main parts, namely transmitter, free space channel, and receiver, where the further breakdown of these main parts is sub-divided into many components [15], as demonstrated in Fig. 2. At the transmitter, an electrical signal is converted to an optical signal by modulating the laser beam. The transmitter includes four basic elements, as illustrated in Fig. 2, namely laser modulator, driver, optical laser source and transmitting telescope, [16].

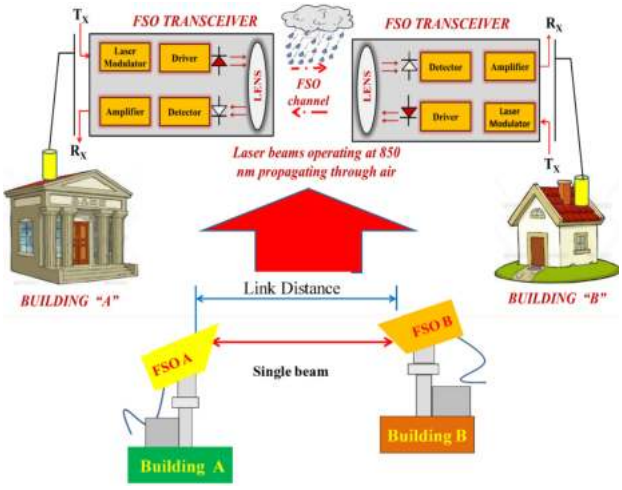

FIGURE 2. Overview of single beam FSO communication system in static placement [18].

A direct modulated laser is used for the modulation purpose, converting the digital data stream into analogue optical signal. The common modulation techniques that are widely implemented are either direct modulation or external modulation techniques [17].

Direct modulation technique occurs within the laser resonator, and the modulation depends on the changes introduced by the additive input components, which will reflect on the intensity of the laser beam. In the case of the external modulation technique, the modulation process occurs outside of the laser resonator, which depends on both the polarization and the refractive dualism phenomenon. Together with the modulators, there will be a driver circuit that varies the current flow through the light source. The light source can be either a laser diode (LD) or a light emitting diode (LED), however LDs are much preferred due to the coherence, highly monochromatic, and directional properties. In other words, LDs produce light waves with a fixed-phase relationship between the points of the electromagnetic wave. There are three common types of LDs, namely the Fabry-Perot (FP), Distributed-Feedback Laser (DF), and Vertical Cavity

Surface Emitting Laser (VCSEL). The VCSELs are lower in cost with excellent performance compared to FP and DFB lasers [19]. The telescopic lens is used to collect the photon stream sent by LD and transmit digital data into the free space channel.

The next portion of the system after the transmitter is the channel, where the propagation medium for FSO system is the free space atmosphere. This medium is proven to have series of layers of concentric gases all around the universe. There are three primary layers within the hemisphere, which are troposphere, stratosphere and mesosphere. These layers are distinguished according to the respective temperature gradients relative to the altitudes. Among the layers, the FSO communication channel transmits within the troposphere. The troposphere is the region where most of the atmospheric phenomenon takes place, such as; physical abstractions, scintillation, geometrical losses, absorption, and atmospheric turbulence [20].

After signal propagation through the FSO channel, an optical receiver is used to receive and process the signal. The optical receiver comprises of five basic components; receiving telescope, filter, amplifier, detector and finally demodulator, as can be seen in Fig. 2. Telescope is used to collect and focus the incoming optical light from channel towards the photo detector (PD). Aperture of large detector telescope is highly required to receive multiple uncorrelated radiations and subsequently perform averaging and focus the radiation to the PD. The averaged signal is then coupled into optical filters to filter the unwanted wavelength components and minimize solar illumination significantly [21].

The detecting portion within the photodetector is performed by a photo diode, which is a semiconductor device that converts the photon energy of the light into an electrical signal by releasing and accelerating current conducting carriers within the semiconductors. The two most commonly used photodiodes are the pin photodiode (PIN) and the avalanche photodiode (APD). The choices are limited only to two types due to their good quantum efficiency, semiconductor design, and widely available from commercial-off-the-shelf (COTS) [22].

In general, FSO receivers can be designed with amplifiers for many benefits as follows:

- The optical preamplifier can be used to boost optical signal strength, which is attenuated due to various atmospheric conditions,
- To overcome the eye-limit restrictions on transmitted laser power,
- To suppress the limiting effect of the receiver thermal noise generated in the electronic amplifier, thereby improving the receiver sensitivity effectively.

The demodulator is designed according to the symbol-set used by the modulator. Its function is to determine the phase of the received signal and map it back to the symbol that it represents, and in the process original data will be recovered. However, the process requires the receiver to be able to compare the phase of the received signal to a reference signal [23].

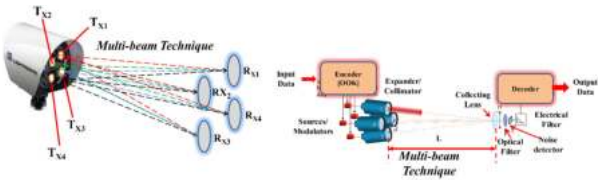

FIGURE 3. Multi-beam FSO system [7].

Finally, in the demodulator side, the pulse received is integrated over one-bit period which is followed by sampling and comparing process to a threshold value to decide a 'one' or 'zero' bit. This is known as the maximum likelihood detector, which reduces the bit error rate (BER) to the minimum [24].

B. CLASSES OF FSO SYSTEMS

FSO systems are categorized into two types, FSO system with single beam and FSO system with multiple-beams. The systems categories have positive and negative attributes. Multi-beam beam FSO system is shown in Fig. 3, where the goal is to transmit data through one beam only. The main drawback of a single beam FSO system is that the beam will be scattered while travelling in free space, which is due to atmospheric turbulence arising from big seized raindrops or haze. Therefore, the probability of beam reaching the receiver is very low in these situations, as a solution, multiple beams are used to increase the probability by assuring at least one of the multiple beams to reach the target, as shown in Fig. 3 [7]. Despite the drawbacks in single beam system, but it is a cost-effective design due to its simplicity and quick alignment between transmitter and receiver [25]. Laser beam combination technique implemented in multibeam FSO system reduces degradation of FSO power which results from the effect of the turbulence in atmosphere [26]. Apart from that and in FSO systems, the impact of turbulence in atmosphere can be alleviated by the technique of laser beams combination. One example of which, is applicable to solve detectors beam scattering and loss of power [27]. Regardless of atmospheric losses [28] the functionality of multi-beam FSO system was evaluated in terms of geometrical losses, link margin and received power [29]. Such system provided a ''fail-safe'' state and furthermore mitigated the impacts of sporadic physical obstructions such as scintillation, snow, rain, insects and birds [7]. Multi-beam system, in particular, is also found to ensure better link availability in coastal regions where low visibility due to coastal fog is considered indeed a localized phenomenon [30].

Investigation into the geometrical losses for single beam, two beams, three beams, and four beams were calculated in [7], and resulted in 27.959 dB, 24.92, 23.20, and 21.938 dB, respectively. As observed from the results, increasing the number of beams resulted in better performance for the FSO system. In addition, the investigation was extended to measurement of the received power relative to BER at varying link distances of 800 m to 1200 m, at data rate of 1 Gb/s for both single and multi-beams FSO systems. As a result,

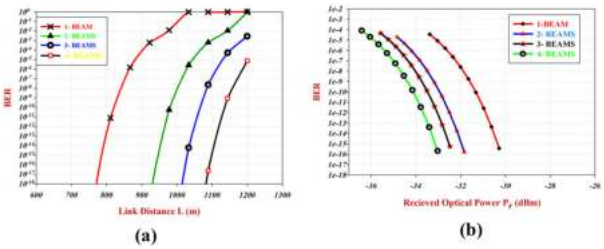

FIGURE 4. a) Optimum link distance achieved at required BER with 1-beam, 2-beams, 3-beams, and 4-beams FSO systems, and (b) Optimum optical received power at required BER with 1-beam, 2-beams, 3-beams, and 4-beams FSO systems [7].

the multi-beam FSO system with four beams had achieved longest distance of 1140 m at a required BER of 10^{-9}, shown by Fig. 4(a). In the case of one beam, two beams, and three beams FSO systems can transmit up to a link distance of 833 m, 991 m, and 1075 m, respectively.

In Fig. 4(b), the optimum optical received power Pr relative to the BER is shown, where again it is clear that increasing the number of beams proportionally increased the sensitivity of the FSO receiver. In another study, an FSO system performance at 1440 m distance of transmission was measured for one, two, three and four beams, as depicted in Fig. 5. It can be observed that the eye diagram opening improved as the number of beams increased, where the eye for one beam FSO receiver had no opening at all, while four beams demonstrated an acceptable opening. Additionally, the study carried out by [7] showed that multi-beam FSO system performed well compared to single beam FSO system under geometrical loss with no rain attenuation. The received optical power was measured to be −12.2 dBm for multi-beam FSO system compared to −24.3 dBm for a single beam FSO system.

C. TRANSMISSION AND MODULATION SCHEMES FOR FSO SYSTEM

The FSO system primarily use intensity modulation/direct detection (IM/DD). While the information is encoded in changes of the light intensity, a square-low detection is typically used in decoding process [31]. The most optical technique for IM/DD system is on-off keying (OOK) [32]. Although the OOK technique implementation is simple and robust against the nonlinearity, it limits the spectrum efficiency. To increase the spectrum efficiency, the OFDM is used to send data simultaneously on orthogonal subcarriers. The OFDM modulation also increases the robustness to multipath propagation. In addition, the multi-input multi-output (MIMO) technique is used to get more bandwidth and throughput in the FSO system. The optical coding division multiple access (OCDMA) technique is used in FSO system [33]. This scheme has several advantages like flexibility of the channel allocation, asynchronously operative ability, privacy enhancement, and network capacity increment. However, the OCDMA technique still suffer from its complexity and cost. The optimization for FSO system can be implemented by using ODM system which provides high data rate, high scalability in terms of number of users and link budget, and robust against rain attenuation [34].

Another new hybrid modulation scheme called pulse position modulation (PPM) and minimum shift keying (MSK) subcarrier intensity modulation (PPM-MSK-SIM) shown in Fig. 6 is proposed by [35].

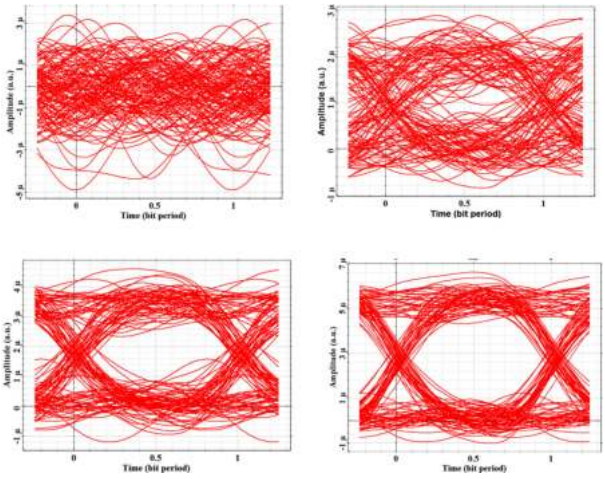

FIGURE 5. Eye diagrams of the FSO received signals at the distance of 1440 m for (a) one beam, (b) two beams, (c) three beams, and (d) four beams [7].

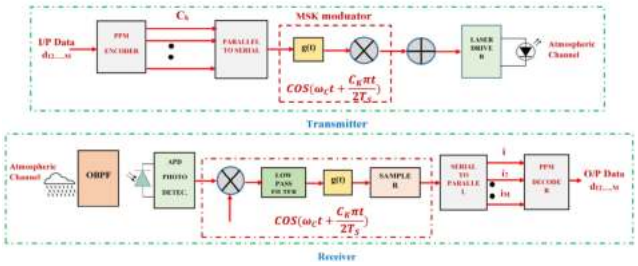

FIGURE 6. Block diagram of FSO communication systems using PPM-MSK-SIM [35].

The proposed modulation technique is based on PPM and MSK-SIM and combines the advantages of MSK's strong anti-interference and PPM's high-power utilization ratio concurrently. The hybrid modulation technique proposed by [35], investigates the BER performance in detail over lognormal atmospheric turbulence channels using APD detector based on simulation. It was realized that the BER performance of PPM-MSK-SIM appeared to be better compared to PPM and BPSK-SIM; the results of the numerical simulation showed that PPM-MSK-SIM has the advantages of improving the BER performance compared with BPSK-SIM and PPM. For example, at the same received irradiance of −2.1 dBm and the same strength of turbulence the BER performance of 2-PPM-MSK-SIM can decrease to whereas those of 2-PPM and BPSK-SIM are just and respectively. This leads the PPM-MSK-SIM to be a promising candidate for FSO modulation technique in future FSO communication systems. These modulation techniques will be modulated onto the optical carrier of an FSO system by exploiting the

frequency, amplitude, phase, and polarization factors. The most commonly used schemes at the optical layer are the intensity modulation with direct detection [1] (IM-DD) and phase modulation in combination with a (self-) homodyne or heterodyne receiver IM-DD is widely adopted due to its simplicity towards implementation.

Literature survey explores a new modulation technique used in FSO communion systems, known as hybrid modulation techniques. A hybrid polarization division multiplexed-differential phase shift keying-multi-pulse pulse position modulation (PDM-DPSK-MPPM) scheme is used in multi-hop free-space optical (FSO) communication systems as suggested by [36]. The results provided by [36], shows that both multi-hop and hybrid modulation schemes are efficient techniques to enhance the performance of FSO links. From the point of view of the bandwidth-utilization efficiency and reliability of the system the hybrid scheme resulted to be more efficient as compared to the traditional binary phase shift keying (BPSK) and MPPM. Compared with the coherent demodulation of PDM-QPSK-MPPM, the hybrid system complexity is reduced at the cost of the degradation of BER performance, which can improve the appropriateness of hybrid modulation technology in FSO system.

In FSO systems the Multi-hop transmission is an alternative relay-equipped technique. In this technique number of relay nodes between source and destination are installed in a sequence manner [36]. Each relay node receives the signal and decodes it. The decoded signal is then transmitted to the next node, this process continues till the receiver receives the signal. The purpose of using number of relay nodes was to mitigate the effect of turbulence and improve the reliability of the FSO link. The hybridization has modulated the laser signals from different aspects and has improved the bandwidth-utilization efficiency and the BER performance of the FSO system.

1) FSO OUTPUT QUALITY AND RESPONSE BASED ON DIFFERENT MODULATION TECHNIQUES

There are many modulation techniques used in the FSO system as mentioned in earlier section. It is much important to understand the impact of these techniques on quality and response of FSO system while installing these systems. Table 1 demonstrates the different types of qualities and system response of FSO system resulted in using the different modulation schemes [49]. In this section a survey on the different modulation techniques which is used in the free space optical communication to improve the performance level of the system is carried out. From Table 1 it can be concluded that all the modulation techniques have their own perspective of advantages and disadvantages. Some techniques are good in energy efficiency and some are good in power efficiency. Selection of definite modulation scheme mainly dependents on the situation and location where the FSO is to be installed and which modulation technique is required by the user [50].

TABLE 1. Output quality and response of FSO system vs modulation scheme.

Sl No.	Modulation Scheme Used	Ref.	Output Quality and Response of FSO System
1.	OOK	[37], [38]	Adaptive threshold, low power efficiency, low cost, ease to implement, binary technique, moderate SNR, highly sensitive.
2.	PPK	[37], [39]	Synchronous, energy efficient, average power is more than MPPM, dynamic threshold not required
3.	MPPM	[37],[40]	Improved PAPR, high spectral efficiency, low peak power.
4.	DPPM	[40]	Higher spectral efficiency compares to the MPPM, improved power efficiency than PPM
5.	PWM	[41]	High average width and spectral efficiency as compare to PPM, better response towards ISI, low power efficiency than PPM, synchronous
6.	DPIM	[37], [41], [42]	No requirement of synchronization, large bandwidth as compare to PPM and PWM, difficult to demodulate
7.	SIM	[37], [42], [43]	Adaptive threshold, high throughput than OOK, less phase fluctuation, more capacity, low power efficiency, less costly.
8.	OOFDM	[43]	Highly resist toward ISI, long range, difficult to combine.
9.	M-ASK	[44]	Less sensitive compare to OOK
10.	PAM	[45]	Higher spectral efficiency, more complex to implement, moderate power efficiency.
11.	MPAM	[46]	Higher spectral efficiency compares to PAM, required dynamic threshold at destination
12.	QAM	[42], [45]	Higher intensity, more power and spectral efficiency as compare to PAM.
13.	BPSK	[37], [39]	Power efficient as compare to QPSK
14.	QPSK	[37], [47]	High capacity, low power efficiency, high spectral efficiency.
15.	DPSK	[46], [47]	More capacity, less data rate as compare to the DQPSK, less spectral efficiency
16.	DQPSK	[47]	Higher data rate, high bandwidth efficiency, low power efficiency
17.	CAP	[48]	More energy efficient as compare to the PAM, less costly, simple implementation

D. FREE SPACE OPTICAL NETWORKS

FSO system is highly used nowadays in every communication system therefore FSO networks becomes a hot topic for investigation and employment for networks that may cover a link distance from a few meters to over thousands of

kilometres [51]. Based on the locations of optical transmitters and receivers and network range of any FSO system [51], FSO networks can be roughly categorised as three main types: (i) Optical Wireless Satellite Networks (OWSNs), (ii) Optical Wireless Terrestrial Networks (OWTNs), and (iii) Optical Wireless Home Networks (OWHNs. It may not be easy to precisely describe these networks, since various FSO subnetworks are integrated into these main networks and operated as a whole, as it is demonstrated in Fig. 7. Each category of FSO network is explained in the following section, and their characteristics are summarized in Table 2.

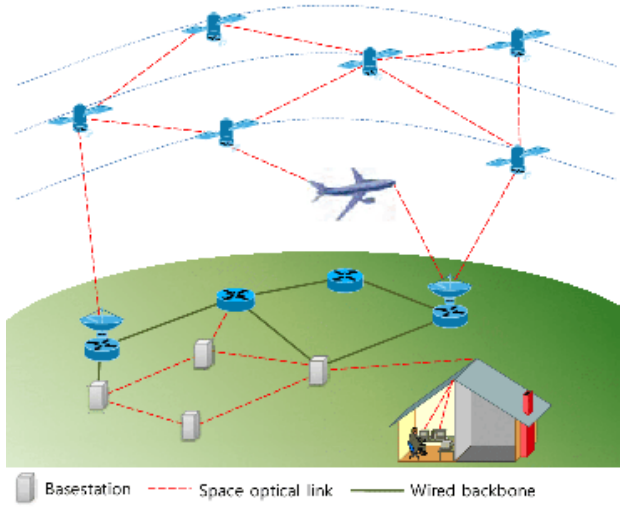

FIGURE 7. The conceptual topology of integrated optical wireless satellite, terrestrial, and home networks [52].

1) OWSNS (OPTICAL WIRELESS SATELLITE NETWORKS)

The OWSNs are designed in such a way that these networks provides a high-bandwidth, optical wireless network access to end-users by making use of space satellites, which cover large areas of the earth [51], [53], [54]. These networks provide a global space backbone network with optical links as demonstrated in Fig. 7, because satellites can support any terrestrial residents regardless of topographical limitations as long as a Line-of-Sight (LOS) is available. As a result, OWSNs offer high quality data services even to isolated areas such as an island, a remote farm, a ship on the ocean, an aircraft, and so forth. OWSNs consist of different types of free-space optical links including inter-satellite, satellite-to-air, and satellite-to-surface optical links. Inter-Satellite Links (ISLs) are designated for routing data traffic hop-by-hop through satellites toward a final destination satellite that has up-and-down links between the aircraft or a ground station on the surface of the earth.

2) OWTNS (OPTICAL WIRELESS TERRESTRIAL NETWORKS)

OWTNs, is known as outdoor FSO networks, which establishes a point-to-point and LOS optical wireless connection between two FSO systems through outdoor atmospheric turbulence channels [11], [55]–[57]. Due to the LOS requirement of FSO system, the distance covered by Laser light propagating through atmosphere may reach hundreds of meters up to tens of kilometres. This FSO model of telecommunication has tremendous potential for wireless communications and is becoming an important means of broadband Internet access.

3) OWHNS (OPTICAL WIRELESS HOME NETWORKS)

OWHNs, also known as indoor FSO networks, are desirable within houses and offices for wireless broadband communications. OWHNs are used to create a LAN made up of cells, where each cell is one of the building's divided spaces [11], [51], [58]–[60]. Typically, each cell has a base station connected to multiple terminals with short-range optical wireless connections such as infrared and LED (light emitting diode). Infrared and LED beams do not penetrate walls, unlike radio waves. Every optical wireless cell should be confined to a room and must be linked to a broadband backbone infrastructure and integrated with it. Of cell is usually free of interference from neighbouring cells. The same beam parameters are reused as a result. We further classify the indoor FSO network into two groups on the basis of various propagation modes: LOS links and non-LOS links, also known as diffused links. A LOS connection requires a clear path between the receiver and the transmitter. LOS connection can be easily blocked by any unforeseen obstacles between the transmitter and the receiver. Compared with Non-LOS links, due to a better power budget and the absence of multipath propagation effects, LOS links achieve better and greater capacity. However, to support mobile terminals with LOS connections, a beam-steering mechanism is necessary. A diffused light source is used in Non-LOS connections to spread a light beam inside a room to take advantage of multiple path propagations induced by reflections in a confined space from all kinds of surfaces, such as furniture, walls, ceilings, and floors. As a consequence, when facing barriers, non-LOS ties are more stable. There is a trade-off, however between network capacity and link reliability here. Usually, compared to LOS connections, a diffused link supports a lower data rate.

E. FSO PARAMETERS

There are two system parameters for FSO which are considered as internal and external parameters.

1) INTERNAL PARAMETERS

These parameters are concerned with the FSO system and are categorized as follows:

a: LINK MARGIN

One of the key aspects of system design is to synthesize a precise link budget, which determines how well an FSO link will operate under certain given weather conditions [61]. In other word, link budget is applied to estimate the margin or excessive power in a link assuming a specific operating condition. This extra available power is then coupled with

TABLE 2. Characteristics of optical wireless satellite, terrestrial and home networks [51], [52].

Sl No.	Network Characteristics	Types of Optical Networks			
		OWSNs	OWTNs	OWHNs (IrDA)	OWHN (MSD, White LEDs)
1.	Location	Orbit	High/open place	Indoor	Indoor
2.	Link distance	~84,000 kilometres	~10 kilometres	~a few meters	~tens of meters
3.	Channel	Vacuum channel	Air turbulent channel	Weak turbulent channel	Weak turbulent channel
4.	RX/RX FOV	Very narrow	Narrow	Limited power for eye and LOS blockage safety	Wide
5.	Performance limiting factor	Misalignment with long distance	Atmospheric turbulence	Lightweight, portable, and inexpensive component	Limited power for eye safety and multipath propagation
6.	Hardware requirement	Precise PAT technology (Ex. Automatic steerable gimbals/beam)	Turbulence-resistant design (Ex. Spatial Diversity, RF/FSO, Hybrid architecture)	Lightweight, portable and inexpensive component	Backbone between cells and MSD–holographic optical diffuser
6.	Miscellaneous	Long Distance coverage to maintain	Various impairment factors	Short-range point-to-point link	Exploiting reflection

a static model of atmospheric attenuation to evaluate the predicted available power concluded from the losses induced by free space. Formation of link budget equation is an important step prior to properly configure an FSO system. The link margin expression parameters of the FSO system shown in Fig. 8 commonly consists of transmitted power, detector sensitivity, power losses in an optical system, geometrical and alignment losses, as described [62] by.

$$LM(i,j) = P_e(i) - S_r(j) - \alpha_{tgoe}(i,j) - \alpha_{atmo}(i,j) - \alpha_{sys}(i,j) \quad (1)$$

where $P_e(i)$ and $S_r(j)$ are the ith transmitter power and the jth receiver sensitivity, while $\alpha_{tgoe}(i,j)$, $\alpha_{atmo}(i,j)$ and $\alpha_{sys}(i,j)$ are represent geometrical attenuation, atmospheric attenuation, and system losses, between link (i, j) respectively. These parameters $\alpha_{tgoe}(i,j)$, $\alpha_{atmo}(i,j)$ and $\alpha_{sys}(i,j)$ were given as following expressions,

$$\alpha_{tgoe}(i,j) = \frac{S_t(i)}{S_c(i)} \quad (2)$$

$$\alpha_{atmo}(i,j) = \alpha_{rain}(i,j) \times d(i,j) \quad (3)$$

$$\alpha_{rain}(i,j) = 1.076 \times R^{0.67} \quad (4)$$

where $S_t(i) = (\pi/4)(d(i,j)\theta)^2$ is the illumination area, θ is the angle of the light beam divergence, $d(i,j)$ is the distance between i and j, $S_c(i)$ is the receiver capture area, and R is intensity of the precipitation.

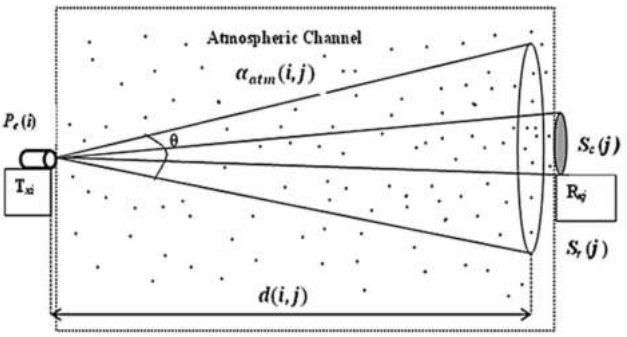

FIGURE 8. FOS model [62].

Based on (2), (3), and (4) the FSO link key collective quality parameter LM can be represented as:

$$LM(i,j) = P_e(i) + |S_r(j)| - \left[10log_{10}\alpha_{tgoe}(i,j)\right] - \left[\alpha_{rain}(i,j) \times d(i,j)\right] - \alpha_{sys}(i,j) \quad (5)$$

b: TRANSMITTED POWER AND DETECTOR SENSITIVITY

The amount of transmitted power is the optical energy launched by the FSO system. Whilst, the detector sensitivity is defined as the minimum magnitude of optical input that produces a certain output energy having a specific BER at the FSO system receiver [63]. These two parameters are normally evaluated in the form of either peak or average power, while the measurement point can be at the transmitter

(laser source) or detector (FSO receiver) apertures. However, while recording the measurement from on laser or receiver spots, it is essential to include any additional losses, which is a loss incurs by the optical power that propagates through the entire system.

c: TRANSMISSION BANDWIDTH & WAVELENGTH

There are new results derived from the research in the field of Free Space Optics (FSO) for the qualification of different wavelengths with reference to future communication (including space) are presented [64]. The contribution deals with a thorough discussion of the different optical wavelengths used either for terrestrial as well as for near-Earth and deep space FSO links. Practical results of COST Action IC-0802 are implemented in the modelling of the FSO channel under deteriorating conditions like rain, snow, dust, fog, clouds and other atmospheric effects. It is intended to interconnect well-proved technologies like 850 nm and 1064 nm as well as 1550 nm wavelength with new technologies under development like 10 μm wavelength. Quantum Cascade Lasers (QCLs) are currently experiencing a strong progression [64].

d: BIT ERROR RATE (BER) IN FREE SPACE OPTICS SYSTEM

The FSO system performance can be evaluated in many ways such as by analysing the BER and Q-factor. BER can be defined to be the ratio of the number of bit errors detected in the receiver and the number of bits transmitted by the transmitter. High value of BER occurs as the result of incorrect decisions being made at the receiver due to the presence of noise (unwanted signals) on a digital signal. Typically, as a quality factor, Q is a one of the essential indicators to determine the optical performance by which to characterize the BER [65]. Both signal to noise ratio (SNR) and bit error rate (BER) are used to evaluate the quality of optical communication systems. BER performance depends on the average received power, the scintillation strength, and the receiver noise. With proper aperture design averaging the received optical power could be enhanced and increased as well as reducing the effect of the scintillation. The SNR with turbulence in terms of the mean signal and noise intensity I0 and In, is given as with taken into account the approximation suggested by [66].

$$SNR(dB) = 10\log\left[\frac{1}{0.31C_n^2\left(\frac{2\pi}{\lambda}\right)^{7/6}L^{11/6}}\right] \quad (6)$$

where λ is the wave-length, L is the link distance between transceiver and C_n^2 is the index of refraction structure parameter. C_n^2 is assumed to be constant with average value of 10^{-16} to 10^{-13} for weak to strong turbulence respectively [67].

e: OPTICAL SYSTEM AND POWER LOSS

In more details, losses in an optical system involve scattering, absorption, surface reflection, and overfull losses. On the other hand, when optical beam travels from transmitter to receiver it spreads causing degrade in power, this phenomena of power loss is known as geometrical loss [68]. In any FSO link, the geometrical loss is entirely influenced by the optical transmitters' beam width, path length of the transmitter, and the area of detector aperture as illustrated in Fig. 9. The power of transmitter P_t which is transmitted over a total area of $\pi(l\theta)^2/4$ [63], while the density of power flux at the detector is $4P_t/\pi(l\theta)^2$ [63] and the detected power can be calculated as $P_r = 4A_rP_t/\pi(l\theta)^2$ [63].

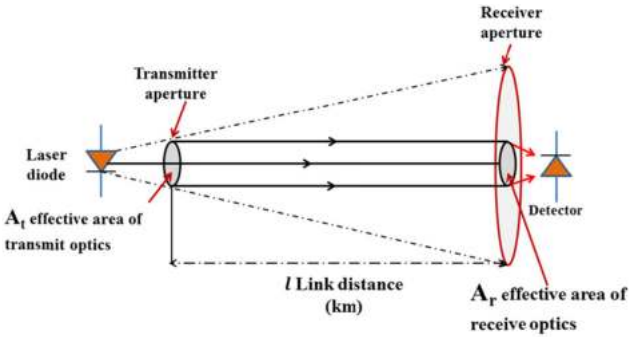

FIGURE 9. Spreading of the transmitted beam in free space between the transmitter and the receiver of an FSO system [63].

Typically, the beam spreads to a radius larger than the receive aperture, and this results in the overfull energy to vanish, where Fig. 10 demonstrates the beam spreading by 0.2 mrad over a 1 km link range.

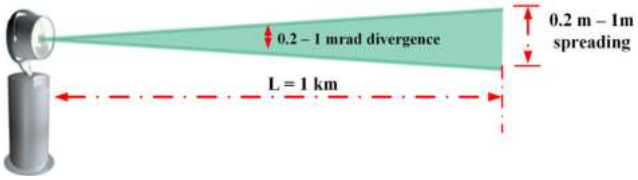

FIGURE 10. Beam Transmission over a 1 km range.

In order to minimize geometrical losses, the multi-beam FSO system, large detector apertures, or small transmission divergence are used. In general, for a single and multi-beam FSO system under a uniform transmitted power distribution that uses a non-obscured transmitter and detector, geometrical losses are evaluated by applying the following formula [9]:

$$A_{geo}(dB) = \frac{P_r}{p_t} = 10\log_{10}[4(A_{RX})/\pi(\theta l)^2] \quad (7)$$

$$A_{geo}(dB) = 10\log_{10}[4(A_{RX}.N_{RX})/\pi(\theta l)^2]. \quad (8)$$

where, P_r is the received power that is equivalent to $4A_{RX}P_t/\pi(\theta l)^2$, P_t is the power transmitted that is equivalent to $\pi(\theta l)^2/4$, A_{RX} is the area of detector aperture, N_{RX} is the amount of detectors employed, θ is the transmitters' beamwidth, and l is the length of link between transmitter and detector that is computed in terms of km.

f: ALIGNMENT LOSSES

Since FSO system operates in wireless medium with narrow-beam (Gaussian distribution) transmitter, alignment loss can be quite common due to inadequate alignment between the transmitter and the receiver [61], [69]. The condition of alignment in an FSO system can be well-achieved when the Gaussian power distribution centre is situated at the detectors' centre. However, loss incurs when the detector is not perfectly aligned with the transmitter as shown in Fig. 11. This is because the detector will not be able to precisely collect the light by the beams edges where the light intensity is quite low. In a practical FSO system, the primary reason for misalignment is the base motion (building sway) of buildings, especially for FSO systems that are installed on skyscrapers, where these buildings are heavily subjected to sway [69], [70].

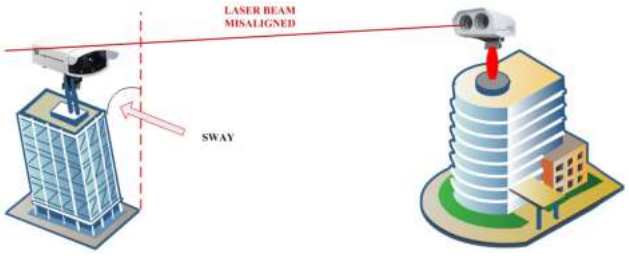

FIGURE 11. Building swaying effect towards an FSO system.

To minimize the misalignment loss, an automatic pointing and tracking system can be integrated into an FSO system, where this tracking system consistently adjusts the FSO system for optimal alignment, as shown in Fig. 12.

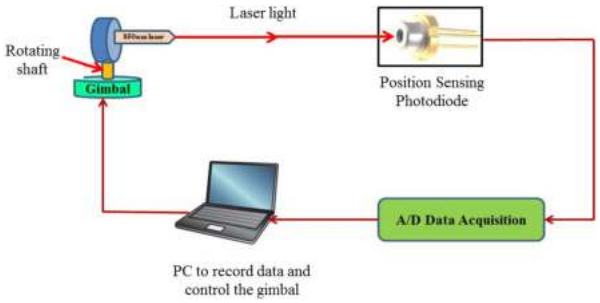

FIGURE 12. Auto tracking for an FSO system to avoid misalignment [52].

As illustrated in Fig. 12, a helium-neon laser is mounted on a gimbal. In order to measure the repeatability and accuracy of the gimbal, an X and Y Duo Lateral Position Sensing Photodiode (PSD) coupled with a preamplifier circuitry are used. The PSD preamplifier circuitry provides bipolar voltage output of the X and Y positions of the centroid laser spot and as well as the total X and Y currents, which are used to normalize the outputs externally to exclude the dependency of the PSD towards the light intensity. The output from the PSD module is recorded via a data-acquisition module and passed on to a computer for computation and control of the movement of the gimbal as desired [71].

2) EXTERNAL PARAMETERS

The external parameters are linked with atmospheric conditions and the losses occurred due to these conditions. The performance of a FSO link primarily depends on the climatologic and the physical characteristics of its installed location [72] as demonstrated by diagram given in Fig. 13. In general, weather and installation characteristics also impacts on FSO link performance [73], by reducing or eliminating visibility, namely atmospheric attenuation, scintillation, window attenuation (if the FSO transceiver is installed behind a window pane), alignment or building motion, solar interference, and line-of-sight obstructions [61]. In order to understand further, this section will describe the atmospheric attenuation arising within tropical regions due to its atmospheric conditions, including rain and haze.

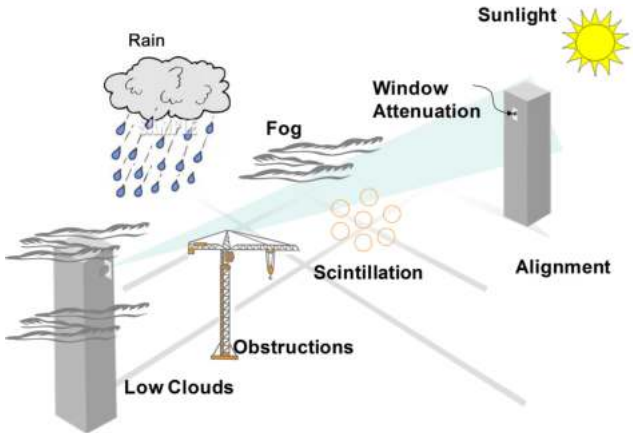

FIGURE 13. Different physical and weather condition effect on FSO link [20], [71].

a: RAIN

The atmospheric parameters, such as absorption, scattering and non-selective scattering have a significant effect on FSO modulated light moving over free space [16]. Absorption based attenuation strongly depends on the wavelength characteristic, where the most severe absorption occurs for wavelengths within the ultraviolet region (below 200 nm). Apart from that, light scattering also strongly depends on the wavelength characteristic, where rain introduces non-selective scattering due to large sized rain particles [74]. In the case of European region, the climate is prone to fog and heavy snow, which directly affects a FSO link [7]. However, in Malaysia, which is located within tropical climate, snow does not exist, fog is not a considerable concern, whereas haze and heavy rain are foreseen to significantly impact the availability of a FSO link [75].

CONVECTIVE AND STRATIFORM RAIN CONDITIONS

Stratiform and convective are the most common types of rain conditions. Stratiform rain precipitates from "nimbostratus

TABLE 3. Rain climatic zones [rainfall intensity exceeded (mm/h)] [85].

Exceedance probability	Rain climate zone														
	A	B	C	D	E	F	G	H	J	K	L	M	N	P	Q
1.0	0.12	0.5	0.7	2.1	0.6	1.7	3.0	2.0	8.0	1.5	2.0	4.0	5.0	12	24
0.3	0.8	2.0	2.8	4.5	2.4	4.5	7.0	4.0	13	4.2	7.0	11	15	34	49
0.1	2.0	3.0	5.0	8.0	6.0	8.0	12	10	20	12	15	22	35	64	72
0.03	5.0	6.0	9.0	13	12	15	20	18	28	23	33	40	65	105	96
0.01	8.0	12	15	19	22	28	30	32	35	42	60	65	95	145	115
0.003	14	21	26	29	41	54	45	55	45	70	105	95	140	200	142
0.001	22	32	42	42	70	78	65	83	55	100	150	120	180	250	170

clouds'', whilst convective rain usually drops from ''cumulus and cumulonimbus clouds'' [76].

Stratiform Type of Rainfall: Posterior weather systems cause this type of rainfall. This kind of rain concentrates in low pressure areas, where warm air encounters cool air. Generally, strigiform can be hardly identified in a fixed rain rate threshold (5mm/h) and it is the most widespread rainfall. It occurs within clouds that are developed horizontally rather than vertically, an example of which is the nimbostratus clouds [77].

Convective Type of Rainfall: Convective rainfall is formed by convective clouds. Such clouds originate from a moisten atmosphere that is over heated in comparison to surroundings temperature. The latter results in a momentous upward movement [78]. However, this type of rainfall occurs due to highly unstable atmosphere which is typically distinguished by heavier and larger particles of rain. This condition can also be specifically characterized in a short time period, having a higher rainfall rates than 10 mm/h [78].

RAIN CELL SIZING

The rain cell is defined as the region of space, which consists of linked points, where the rainfall rate exceeds a predefined threshold. Many studies investigated the size and shape of rain cells via radars [79]–[81]. Furthermore, there are other studies carried out by using long-term time series measurements by using weather stations combined with time integration over a minute, which are used to estimate rain cell sizes by applying the synthetic storm technique [82].

In [83], it is found that the statistics of rain cell geometry are independent of their location and threshold, with an average elasticity factor of 0.5. Based on elasticity, it is assumed that, on average, rain cells are twice as long as their width.

RAIN CLIMATIC ZONES

Since FSO system is prone to rain and its absorption characteristic, hence understanding the rainfall rate is paramount, which is defined by International Telecommunication Union (ITU)-R and the scientific community. Currently, the new recommendations (e.g. P.837-6) [75], [84] include highly precise models to predict the rain rate statistics according to regions throughout the world. Globally, rainfall is subdivided into fifteen climatic zones by ITU according to the rainfall intensity of (mm/hr) for each region. These readings are highly important in calculating specific attenuation relative to rain. Table 3 illustrates the ITU climatic zones [85]. Malaysia is classified under P region specifically for Microwave technology, however, it is useful as a reference to model the rain attenuation factor for FSO [86].

RAINDROP SIZE DISTRIBUTION (DSD).

The raindrop size distribution (DSD) can be expressed as, which defines the concentration value of raindrops with equal-volume diameter (mm) in a given volume of space. The DSD parameter plays an important role in calculating the rainfall rate and the relative signal attenuation for both radio wave and FSO systems [87]. Naturally, DSDs may compute varying values for the same rain intensity. As an example, large number of small drops may result in the similar rain intensity as the small number of large raindrops, although both scenarios fall under two very different categories of DSDs [88]. Similarly, two different categories of DSDs with the same intensity may result in two different values for signal attenuation [77]. Previous studies have proposed a number of analytical expressions for DSD distributions [89], where the exponential distribution is proposed by [90], lognormal distribution is proposed by [91], the gamma distribution is proposed by [92], and the normalized gamma distribution is proposed by [89]. The investigation of DSD is typically carried out by fitting the analytical form onto the measured DSD data. The resultant parameters of the analytical distribution can be compared to the meteorological data for verification.

As suggested by [93], the Marshall and Palmer analytical form of DSD is widely accepted by many, and is a good representation of the DSD for a long period of time. Thereafter, the exponential distribution is established by [90] with new results. Recent studies, including [93], [94], have anticipated the DSD as a substitute for analytical distribution.

ATTENUATION

In the absence of fog, atmospheric scattering is primarily caused by rain attenuation in tropical areas. It is commonly classified into Mie, Rayleigh and non-selective scatterings. Mie scattering is applicable to particles that have comparable

sizes in wavelength, a good example is the water droplets in both fog and haze [95]. While, Rayleigh scattering takes place when size of a particle is smaller compared to wavelength, however, at 1550nm wavelength, its impact is insignificant. Non-selective scattering, on the other hand, happens when drop size of a particle is larger than wavelength, this sort of scattering is wavelength independent [74]. In FSO system, rain impact is characterized as a distance- reducing. It is therefore categorized as non-selective scattering due to rain drop radius of (200-2000μm).

This is largely bigger than FSO source light wavelength, this concludes that scattering has no significant impact on FSO system [68]. Malaysia, as a tropical region, experiences rain as a dominant factor for signal attenuation due to scattering phenomena. This scenario can lead to signal degradation or even complete loss of signal, because in these regions, rain occurs throughout the year at the rate of $>$ 145 mm/hr for 0.01% average within a year [96], [97].

RAIN ATTENUATION PREDICTION MODEL

The process of developing a rain attenuation model for tropical regions are based on the guidelines proposed by the ITU-R [98]. It is recommended that the rainfall data collection has to be repeated in an interval of 1 minute for precise estimation of the rain rate [98]. The underlying method is based on the relationship between the collected rain rates at mm/h and the relative received optical power [99]. The effect induced by the heavy rainfall towards the performance of the FSO link can be computed by calculating the rain attenuation and the corresponding rain rate [100]. In general, the rain attenuation prediction modelling will be carried out via two methods, namely the empirical method and the physical method [101]. Empirical method is developed by producing a relationship between the observed attenuation distribution and the corresponding observed rain-rate distribution that is measured over an integration time of 1 minute [102]. In the case of physical method, the actual physical behaviour of the attenuation process will be taken into consideration [103]. The typical raindrop size distribution model adopted by ITU-R is the Marshal and Palmer's distributions [103]. The model by Marshal and Palmer is based on fitting the measured data relative to the collected data from Laws and Parsons [100]. The rain attenuation is a critical factor in determining the reliability of microwave and millimetre-wave systems. Rain specific attenuation can be expressed via the power law equation [104]:

$$\gamma_{Rain} = k.R^{\alpha} = A_{atmos} \tag{9}$$

where,

γ_{Rain} - rain attenuation (dB/km),
R - rain intensity (mm/hr),
A_{atmos}- atmospheric attenuation,
k and α - rain coefficients.

The coefficients k and α depend on several parameters on, namely the wavelength of the FSO system, the free space temperature, the DSD, and the polarization [105]. The values of these coefficients can be obtained from ITU-R P.838-3 [106].

In order to calculate the rain attenuation, it is common to assume that the raindrops have a spherical shape, hence the estimation of and values are independent of vertical and horizontal polarizations [99]. The values of and based on a prediction models by France (Charbonneau's model) and Japan measurements are recommended by ITU-R, and as well as other models that have been used for FSO rain attenuation prediction [90], [107], as tabulated in Table 2. The values of and proposed by Charbonneau's model is computed via the measurements taken at very low rain rates ($\sim$5 mm/hr), because the measurements originated from Europe, where the rain fall rate is relatively low compared to tropical regions [108]. In the case of tropical regions, the rain rate can reach up to 150 mm/hr, especially during monsoon seasons. In the case of Japan, and values are computed based on measurements recorded at a maximum rain rate of 90 mm/hr, which is significantly lower compared to the average maximum rain rate in tropical region [105]. Both Japan and Europe models did not take into account of the higher rain intensities, which occurs in tropical countries, thus the estimated and values by these models are not applicable in the tropical regions [73]. The values predicted by Marshal Palmer and Joss distributions are based on DSD method [105]. However, [109] suggested that implementing DSD technique in tropical regions will result in severe prediction error. In the study carried out by [96], estimated power law parameters k, and α as 2.03 and 0.74, respectively, for the FSO applications in tropical South-East Asian weather. These parameters are computed by using least square mean equation (LSME) method with Levenberg-Marquardt optimization, where the input data was recorded during heavy rain within a period of a year. As a summary, Table 4 demonstrates a comparison among the parameters produced by various researchers to estimate a specific attenuation arising due to rain.

b: HAZE

Sources such as, dust, smoke and other particles that are distributed in the atmosphere generate particulate matter which is so-called haze [43]. Exposure of these matters to gaseous pollutants leads to certain chemical reactions [110]. Since the size of the haze particles are somewhat comparable to the size of the wavelength of the transmitted signal, the effect is therefore classified as Mie Scattering. According to a data collection conducted by [111], the air in Malaysia can be generally considered as good in quality, the typical visibility distance is therefore more than 10 km throughout the annual. It is worth to mention that fires occurring seasonally within few regions in Malaysia and Sumatra reduce the distance of visibility. Often, this situation lasts for days and occasionally continue to happen for weeks at most. For an example, the previous incidents took place in August 2005, October 2006, and most recently was in July 2018, where the visibility can go as far of dropping below 500 m [111].

TABLE 4. Comparison among parameters used to estimate specific attenuations arising from rain.

Attenuation Model	Location	Environment /Rate of rain *R* (mm/hr)	Expression
Joss [106]	Switzerland	Temperate/light rain (drizzling) R < 3.8	$0.509R^{0.63}$
Joss [106]	Switzerland	Temperate/average rain 3.8 < R < 7.6	$0.319R^{0.63}$
Joss [106]	Switzerland	Temperate/convective rain R > 7.6	$0.16R3^{0.63}$
Marshal-Palmer [99]	Canada	Temperate /rain	$0.365R^{0.63}$
Laws & Parson [100]	---	---	$0.543R^{0.87}$
Charbonneau [93]	France	Temperate	$1.076R^{0.67}$
Japan [93]	Japan	Temperate	$1.58R^{0.63}$
Malaysia [96]	Malaysia	Tropical R > 145	$2.03R^{0.74}$

Therefore, in modelling the FSO link, this particular scenario has been taken into account as an important parameter [111]. Fig. 14 depicts the visibility relative to link distance under the conditions of clear sky, light haze, haze, and fog. Under the conditions of light haze and also fog, and clear sky, Fig. 11 shows the relationship between visibility and distance of link.

c: FOG

The Haze and fog particle consists of a mixture of very fine water droplets or ice near the surface of the Earth [113]. The light is scattered by these particles and hence reduces visibility. Fog is characterized as less than 1 km of visibility and relative humidity that reaches the level of saturation (100%) [113], [114]. Some parameters, such as distribution of particle size, liquid water content (LWC), temperature and humidity, etc. [115], define the fog. The most important parameter is the distribution of the particle size used to model the modified gamma distribution in the literature [114]. The features of the fog can vary from one fog event to another or even during the same fog event. This relies on certain variables, such as season, location, life cycle, etc. [114], [115]. Therefore, to explain each event alone it is important to know the fog parameters, particularly the particle size distribution. In general, the size of the fog particle is comparable to the wavelength of the FSO signal, so for FSO connections it causes great attenuation. The attenuation in thick fog exceeds 480 dB/km and in mild fog 130 dB/km [114]. The visibility range obviously decreases as the fog concentration rises in the air. It is necessary to determine the size and water content of fog particles in order to predict attenuation. This knowledge is however, difficult to achieve and not always available at the installation site of the FSO link. Researchers therefore suggested analytical models that rely on visibility data that is commonly available in cities from meteorological stations. In fact, the origin of fog attenuation models using visibility data stems from the atmospheric visibility concept itself [116]. Visibility is characterised as the distance from an object where the distinction between images drops to a certain percentage of what it would be if the object were instead nearby [113]. In visibility description, image separation that drops to 2 percent and 5 percent is considered. Visibility is estimated at 550 nm, which reflects the maximum solar spectrum strength. The Beer-Lambert (a.k.a. Koschmieder) law can be used for the 5 percent definition of visibility and light beam at 550 nm to achieve the specific attenuation as [115]. Table 5 summarizes the different fog attenuation empirical models with different visibility values with module description.

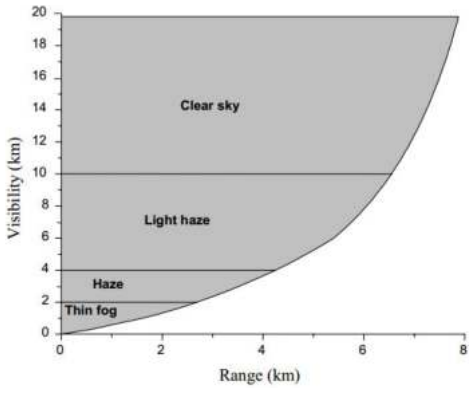

FIGURE 14. Visibility relative to link range achievable at different weather conditions [112].

SPECIFIC ATTENUATION ARISING FROM FOG AND HAZE EFFECTS (MIE SCATTERING)

The performance of FSO system under the fog and haze conditions was investigated by [117] in Malaysia. As indicated by Fig. 15, fog substantially deteriorates the performance of FSO system. However, the investigation conducted by [117] only focused on free space channel with haze and not fog. The former considered fog as not a limiting factor in an FSO system operating in a tropical area. Indeed, this may not be true as haze is foreseen to be of significant influence on performance of an FSO link. The attainable quality of visibility is the most considerable outcome when fog and haze are present. Haze contributes to 1000 m higher visibility in comparison to fog, this is illustrated in Fig. 15. Evaluation of attenuation which arises from fog and haze is commonly referred as Mie scattering parameter [118].

In the presence of complex shapes and orientations with atmospheric particles, Mie scattering theory may be complicated to use [119]. The attenuation caused by scattering is therefore computed by applying an empirical formula that was reported in [4], in which attenuation coefficient is regarded directly to visibility.

TABLE 5. Comparison among different empirical models used to estimate specific attenuations arising from fog.

Module	Formula	Module Description
Kruse [133]	$A=\frac{13}{V}\left\{\frac{\lambda}{0.55}\right\}^{-q}, q=\begin{cases}1.6 & V>50km\\ 1.3 & 6km<V<50km\\ 0.585V^{1/3} & V<6km\end{cases} dB/km$	Kruse proposed a change to incorporate the impact of particles at wavelengths other than 550 nm. For many years, the Kruse model (since 1962) has been commonly used as the specific model predicting the attenuation from visibility data [120]. In accordance with the Kruse model, attenuation is given by 6
Kim [120]	$A=\frac{13}{V}\left\{\frac{\lambda}{0.55}\right\}^{-q}, q=\begin{cases}1.5 & V>50km\\ 1.3 & 6km<V<50km\\ 0.16V+0.34 & 1km<V<6km\\ V-0.5 & 0.5km<V<1km\\ 0 & V<0.5km\end{cases} dB/km$	A analysis of the validity of the Kruse model by Kim proposed modifications to the visibility parameter of less than 500 m for this model [120]. The suggested Kim model (2001) considered fog attenuation for V<500 m as wavelength independent, based on Mie theory calculations. The original coefficient in the Kruse model was updated according to this analysis.
AlNaboulsi Convection [115]	$A=4.343\left(\frac{0.11478\lambda+3.8367}{V}\right) dB/km$	In the previous models, information about particle size distribution and fog type was not included in deriving the model. The authors in [115] considered this issue. Instead, a FASCOD programming tool has been used to model fog attenuation. The software is based on Mie scattering theory with modified gamma distribution for fog. Using this tool, Al Naboulsi [115] derived a model (2004) for fog attenuation in the spectral band 0.69–1.55 km which is valid for visibilities between 50 m and 1 km. Two models of attenuation prediction for convection and advection fog types have been proposed.
AlNaboulsi Convection [115]	$A=4.343\left(\frac{0.18126\lambda^2+0.13709\lambda+3.7502}{V}\right) dB/km$	
Ijaz [134]	$A=\frac{17}{V}\left\{\frac{\lambda}{0.55}\right\}^{-q\lambda}, q(\lambda)=0.1428\lambda-0.0947 dB/km$	Due to the difficulty of taking measurements in a real environment, the authors in [134] built a controlled indoor chamber and measured fog attenuation over 0.6 km to1.6 km wavelengths. The results show attenuation wavelength dependency for V>15 m, where the visible wavelengths are attenuated more than infrared wavelengths. Moreover, a new model (2013) was proposed for wavelengths between 0.6km and 1.6km

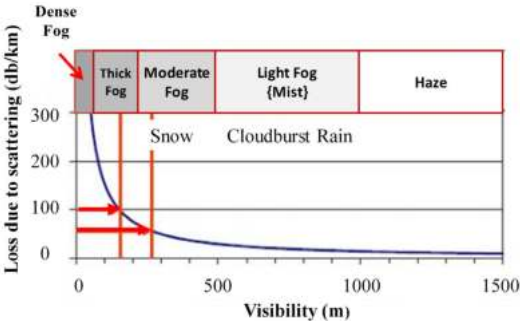

FIGURE 15. Attenuation in atmosphere with regards to visibility [118].

The visual range or in other term, visibility, is commonly defined as the distance where light gradually reduces by 2% in comparison to level of the original power [120]. In order to calculate attenuation due to fog and haze in (dB/km), the empirical formula is given by [118], [119]:

$$\gamma_{(fog,haze)}=\frac{3.91}{v}\left\{\frac{\lambda}{550nm}\right\}^{-q} \tag{10}$$

where v, is visibility which is expressed in km, λ is wavelength with nm as a unit, and q is a coefficient that depends on scattering particles' size of distribution. The parameter q is calculated by applying the theory proposed by Kruse and Kim, as expressed in Equations (11) and (12) which are derived by fitting the experimental results. In the case of large attenuation values, Kim model is preferred.

$$q=\begin{cases}1.6 & \text{if } v>50\text{km}\\ 1.3 & \text{if } 6\text{km}<v<50\text{km}\\ 0.585v^{1/3} & \text{if } v<6\text{km}\end{cases} \quad \text{CRUSE-MODEL} \tag{11}$$

$$q = \begin{cases} 1.6 & \text{if } v > 50\text{km} \\ 1.3 & \text{if } 6\text{km} < v < 50\text{km} \\ 0.558v^{1/3} & \text{if } v < 6\text{km} \\ 0.16v + 0.34 & \text{if } 1\text{km} < v < 6\text{km} \\ v - 0.5 & \text{if } 0.5\text{km} < v < 1\text{km} \\ 0 & \text{if } v < 0.5\text{km} \end{cases} \quad \text{KIM-MODEL} \tag{12}$$

The international visibility codes are shown in Table 6. It can be considered as a reference for FSO system behavioral study [121] for fog and haze conditions.

TABLE 6. Weather conditions international visibility codes [121].

Weather Conditions	Visibility in km
Light Haze	2.8 – 4
Haze	1.9 – 2
Dense Fog	0.0 – 0.05
Thick Fog	0.2
Moderate Fog	0.5
Light Fog	0.77 – 1
Thin Fog	18.1- 20
Clear	5.9 – 10

d: ATMOSPHERIC TURBULENCE

There is another important factor which degrades the optical signal along FSO channel. This factor is atmospheric turbulence. The refractive index variations along FSO path leads to atmospheric turbulence. The optical scintillation then occurs at the FSO receiver [122]. The Rytov variation is usually used to depict the intensity of optical scintillation given by [123]:

$$\sigma_R^2 = 1.23 C_n^2 K^{7/6} L^{11/6} \tag{13}$$

where $K = 2\pi/\lambda$ is the wave number and λ is the wavelength, L is the link distance between transceiver and C_n^2 is the index of refraction structure parameter. C_n^2 is assumed to be constant with average value of $10^{-17} m^{-2/3}$ to $10^{-13} m^{-2/3}$ for weak to strong turbulence respectively. Atmospheric turbulence load

$$= \begin{Bmatrix} weak & if & \sigma_R^2 \leq 0.5 \\ med \rightarrow strong & if & \sigma_R^2 \leq 5 \\ strong - saturation & if & 5 \leq \sigma_R^2 \leq 25 \end{Bmatrix} \tag{14}$$

Fig. 16 demonstrates the probability of outage (P_{out} min) for weak ($\sigma_n^2 = 0.5$), medium ($\sigma_n^2 = 1$) and strong ($\sigma_n^2 = 5$) turbulence strengths at normalized jitter values of $\sigma_{sa} = 3$ and 4. It is clear from the figure that while Ratvo variance moves from weak to strong turbulence the minimum outage probability is achieved by decreasing the laser bandwidth which results in large values of minimum outage probability. If this is the case then the FSO system will have bad performance.

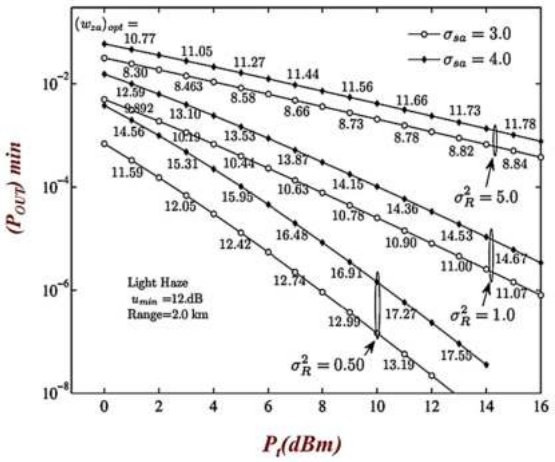

FIGURE 16. Minimum outage probability for weak to strong turbulence and light haze vs. transmitted power [122].

TURBULENCE-INDUCED SCINTILLATION

The theoretical approach of atmospheric turbulence evaluation began several years ago, but it does not agree with the outcome of the experiment presented by. Nevertheless, the operation of the FSO system with an appropriate BER is desirable regardless of the atmospheric turbulence situation. Horizontal propagation research has recently increased to enhance FSO communication systems. Over the years, various statistical models have been developed to describe atmospheric turbulence channels with different intensity strengths. As it offers an excellent agreement between theoretical and experimental data, the K distribution was used as an effective model for strong turbulence channels. The turbulence model given by was used by Uysal and Li to test the output of coded FSO systems in terms of the likelihood of pairwise error and BER. Kaisaleh also analyzed the BER performance of an FSO communication device based on heterodyne over K turbulent fading propagation medium.

Optical Scintillation Losses Estimation: Loss estimation is an important factor for adequate link budgetary, planning and efficient deployment of FSO. Speed and degree of fluctuations (i.e. scintillation frequency) varies with wave frequency. For instance, given a plane wave, a low turbulence, and a particular receiver, the scintillation variance can be expressed as:

$$a_{scin} = \sqrt{23.12 \left(\frac{2\pi}{\lambda} 10^9\right)^{7/6} c_n^2 l^{11/6}} dB \tag{15}$$

λ (nm) is transmitter wavelength in (nm), l(m)represents length of the channel and $c_n^2 \left(m^{2/3}\right)$ is the refer index structure parameter. $c_n^2 = 10^{-16}$ is for low turbulence, 10^{-14} for moderate turbulence and 10^{-13} for high turbulence. This parameter does not have the same figure at optical waves. Optical waves are particularly sensitive to humidity fluctuation and refractive index is a primary varies with varying temperature. Experimental results available today confirm the validity of theoretical results fairly well for the atmospheric layers of

altitudes higher than 50m. For height below 50m, during the daytime, the shape of the structure constant is better approximated by:

$$c_n(z) = r^{-4/3} \tag{16}$$

Hufnagel model provides a good approximation for the optical refractive index structure constant (detailed work from Tatarski's work to the model is shown in. The model can be expressed as:

$$c_n^2(z) = 2.72 \times 10^{-16} \left\{ 3V^2 \left(\frac{z}{10}\right)^{10} \exp(-z) + \exp\left(-\frac{z}{1.5}\right) \right\} \times \left(m^{-2/3}\right) \tag{17}$$

V is wind speed (m/s) and z is the altitude in kilometres. Equations (15) and (17) can be placed side by and expressed as: Equation (18) can therefore be used to estimate optical scintillation losses in the channel of optical links.

$$a_{scin} = \sqrt{\frac{23.17 \left(\frac{2\pi}{\lambda} 10^9\right)^{7/6} 2.72 \times 10^{-16}}{\left\{ 3V^2 \left(\frac{z}{10}\right)^{10} \exp(-z) + \exp\left(-\frac{z}{1.5}\right) \right\} l^{11/6}}} \ (dB) \tag{18}$$

Techniques Used in Reduction of Scintillation Effect on Free Space Optical Communication: As it was noted in the earlier section that scintillation has got a great impact on power degradation of FSO system, so to reduce this effect many researches were carried out. Different researchers used different techniques to reduce this effect, but the most commonly used techniques to reduce this effect are known as coherent-based Homodyne detection technique and Dual Diffuser Modulation (DDM) technique. Using coherent-based Homodyne detection, is an alternative method used in FSO system to reduce the scintillation effect. Homodyne detection is a well-known and efficient way to combine the signal field and a local oscillator reference field through a square law detector that helps to overcome the scintillation effect. The Dual Diffuser Modulation (DDM) technique is a new modulation technique that can produce superior modulation that can decrease the scintillation index, thereby increase the power obtained and the level of the threshold signal. The results analysis of the study carried out shows that free space optics (FSO) can have good power output obtained under heavy turbulence. The DDM provides a better performance as compare with conventional IM/DD-OOK and IM/DD-OOK with diffuser. This can help FSO system to combat with severe turbulence effect for optimum operation.

e: MOLECULAR ABSORPTION AND SCATTERING

As explained earlier, electromagnetic waves are attenuated in free space due to absorption and scattering processes [124], [125]. The process of absorption occurs when a radiated photon is absorbed by gaseous molecules within the atmosphere, consequently either converts the photon into a kinetic energy or re-radiates the energy [49]. It is also important to note that atmospheric absorption is a wavelength dependent phenomena, where the most severe absorption occurs at ultraviolet wavelengths, while little absorption takes place at visible wavelengths of 400 nm to 700 nm [49]. Apart from that, light scattering is also a wavelength dependent phenomenon. Particles, including air molecules, when the size is smaller compared to the wavelength, the resulting outcome will be the Rayleigh scattering effect with symmetrical angular distribution characteristic [49].

At ultraviolet and visible wavelengths, Rayleigh scattering is quite noticeable. On the other hand, the scattering effect for wavelengths that are greater than 3 μm is insignificant, while scattering produced by particles that are comparable in size to a wavelength is known as Mie scattering. Whereas, scattering resulted from particles larger than the wavelengths is known as the non-selective scattering, where one of the examples is the large water droplets [49].

Molecular absorption and scattering effects are often combined and can be expressed as a single attenuation coefficient [24], which can be written as:

$$\gamma(\lambda) = \gamma(a) + \gamma(s) \tag{19}$$

where $\gamma_{(\lambda)}$ the attenuation coefficient at a respective wavelength λ while $\gamma(a)$ and $\gamma(s)$ are the coefficient parameters describing molecular absorption and scattering process, respectively. The transmittance τ of laser radiation that has propagated a distance L considers the attenuation coefficient γ as described by:

$$\tau = \exp[-\gamma(\lambda)L] \tag{20}$$

where, the product γL is termed as the optical depth. Both absorption and scattering effects are deterministic in nature and can be predicted based on a variety of conditions.

III. SCALABILITY OF FSO NETWORK

As discussed in the earlier section, multi-beam FSO system will enhance the link performance by improving the link distance, geometrical loss, and received optical power [126]. However, traditional single beam and multiple beam FSO systems can only operate as a point-to-point system. As a solution, hybrid dense wavelength division multiplexing (DWDM) FSO network was proposed and evaluated [8], [127]. Similarly, the benefits of deploying a single and multiple beam FSO systems combined with DWDM were investigated in [8], [128]–[130]. DWDM technique offers numerous advantages and to name some, the technique allows adequate power budget, passive operating principle, multiplexing ability across many systems without interference, and provides enough margin to support a system with tremendous capacity. Although the FSO is a well-known communication system, the recent effort of combining it with DWDM has brought a new momentum for the communication applications, and thus has increased the potential of providing high speed broadband [131]. One crucial factor found by [100] is that despite having more

than one wavelength in a system, the actual system only experiences a single-beam attenuation effect. In [99], the authors applied the hybrid technique to overcome limitation in received power, limitation in transmission distance, and limitation in scalability, which are pronounced in the ordinary hybrid DWDM/single beam FSO systems under the condition of heavy rain. As a result, the proposed design achieved two-fold benefits, namely an increase in the number of end users (EUs) and decrease in rain attenuation. Such an outcome is highly beneficial to tropical regions, including Malaysia, in minimizing the attenuation impact due to heavy rain for FSO link and concurrently increase the network scalability. One of the other notable studies is the hybrid four channel 1.25-Gb/s DWDM/multi-beam FSO system. This particular system has four wavelengths with standard down link channel spacing of 0.8 nm (100 GHz). It was reported that the hybrid DWDM/multi-beam FSO system improved the performance of the FSO link in the following categories, namely network efficiency and scalability. The proposed technique provided connectivity to four end users, each at a data rate of 1.25 Gb/s with an FSO link distance of 1100 m under heavy rain condition. The general architecture of the proposed hybrid DWDM/multi-beam FSO network that was proposed by [8] is illustrated in Fig. 17.

The Hybrid DWDM/ multi-beam FSO network proposed by [8] shown in Fig. 17, comprises of an FSO base station (FSO-BS), a free space optical channel, an optical distribution node (ODD), and multiple FSO end users (FSO-EUS). At the FSO-BS, the pseudo random bits sequence generator generates data streams, B1, B2 .... BN, that are transmitted into the FSO channel by modulating these streams into multi-beam transmitters, FSOA1, FSOA2, . . . , FSOAN. Whereas the ODD comprised of detector lens, optical combiner, and demultiplexer. Multiple outputs of the ODD are directly connected to the end-users (EUs) units using fiber optic cables.

In the study conducted by [8], it clear that the FSO channel was subjected to heavy rain attenuation and geometrical loss of 19.0 dB/km and 21.94 dB, respectively [7], while the overall measured FSO transceiver loss is fixed at 8 dB. Before exploring further into multi-beam system, it is important to understand that at the point of being transmitted, multi-beam signals are completely independent. However, upon arriving

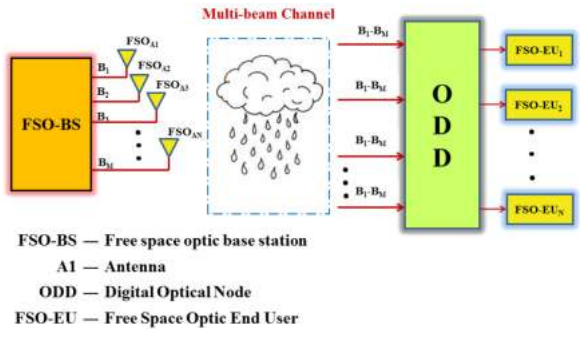

FIGURE 17. Hybrid/ DWDM-multi-beam FSO network architecture [8].

TABLE 7. Comparisons across WDM and DWDM-FSO links.

Reference	[129]	[130]	[132]	[8]
FSO systems types	Single beam	Single beam	Multi-beam	Multi-beam
Beams Number	1	1	4	4
Weather condition	Heavy rain R= 80 mm/hr	Heavy rain R<120 mm/h	Haze	Heavy rain R=150 mm/h
Link distance in m	1500	2400	5300	1200
Wavelength in nm	1550	850	1550	850, 850.2, 850.4,850.6
Transmitted power in dBm	30	10	10	7.7
Geometrical loss in dB	0	0	0	21.938
Atmospheric loss in dB/km	19.28	8.86	0.233	19.00
Data rate in Gb/s/Ch	0.622	0.64	10	1.25
Multiplexer	DWDM	DWDM	WDM	DWDM

at the receiver, the signals will overlap due to the distance travelled and resulting in a single high-powered beam [18]. At the receiver site, the four beams are received by the four receiver optical lenses (Rx). The ODD module combines all the received signals by using an optical combiner followed by a demultiplexer to separate the signals into four high power beams at the rate of 1.25 Gb/s. These four beams are forwarded to the respective users for internet access. Each users/EU is configured with an Avalanche Photo Detector (APD) with a gain of 3 to convert the optical signal to electrical signal and cascaded with one Low-Pass (LPF) Filter to filter the unwanted signals.

The performance of the network depicted in Fig. 18 [8] is demonstrated primarily via bit error rate (BER) measurement. The (BER) against optical received power for the FSO EUs across the four downlink wavelengths (λ_1, λ_2, λ_3, and λ_4) is analyzed for a link distance of 1100 m, as shown in Fig. 18.

At a BER of 10^{-9}, the receiver sensitivity variations for different wavelengths appears to be insignificant, resulting

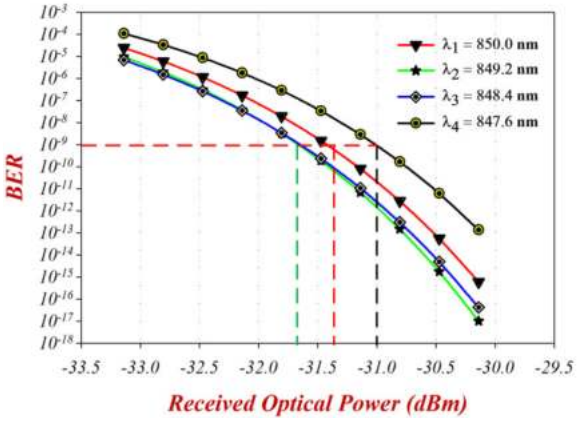

FIGURE 18. BER performance of the received optical power for the FSO EUs.

in less than a ∼1 dB. There are various literatures on hybrid/DWDM FSO network specifically catered for tropical climate. Table 4 summarizes these networks to demonstrate the uniqueness of each of these links.

From Table 7, it is clear that the data rates achieved by each end users are only between 0.622 and 0.64 Gb/s/ch [130], [132] owing to the attenuation that highly affects a single-beam FSO system compared to a multi-beam FSO system. The transmitted power used in the network proposed by [129] is too high, hence not practical in the case of any FSO systems [8].

However, although drawbacks of [100] are largely noted, but it was the only design that achieved a link range of up to 2400 m. This lengthy range is viable because of the lower attenuation within the link, where the rain intensity was lesser than 120 mm/hr. Apart from that, compared to study performed by [8], the effective link attenuation is greater because of the higher rain intensity of 150 mm/hr.

IV. CONCLUSION

A comprehensive review on the emerging technologies for the next generation FSO network was thoroughly explored. The recent developments of single beam and multiple beams FSO systems were widely discussed. Thereafter, the attenuation effects resulted from heavy rain and haze toward the FSO link degradation were explored along with the challenges experienced by the optical beam propagating over the atmospheric link were also explained. For further enhancement, the Multi-beam technology was combined with DWDM technology to enhance the scalability of any communication networks. The hybrid DWDM/multi-beam FSO system was observed as a suitable candidate to be applied for future networks. To successfully deploy these hybrid DWDM/FSO technologies in future networks, the implementation complexity must be minimized so that the capital expenditure will meet the commercial cost. The next generation FSO network requires to be designed with high scalability of reaching up to 16 or 32 channels, which will provide connectivity to 16 or 32 end users.

REFERENCES

[1] H. Henniger and O. Wilfert, "An introduction to free-space optical communications," *Radioengineering*, vol. 19, no. 2, pp. 203–212, 2010.

[2] H. E. Nistazakis, T. A. Tsiftsis, and G. S. Tombras, "Performance analysis of free-space optical communication systems over atmospheric turbulence channels," *IET Commun.*, vol. 3, no. 8, pp. 1402–1409, Aug. 2009.

[3] L. Dordova and O. Wilfert, "Optimal laser diode operating mode with unstable operating temperature in turbulent atmosphere," *Proc. SPIE Semicond. Lasers Laser Dyn.*, vol. 6997, May 2008, Art. no. 69971G, doi: 10.1117/12.779731.

[4] W. R. Bradford, "Laser beam propagation in the atmosphere," *Opt. Laser Technol.*, vol. 16, no. 5, p. 274, Oct. 1984.

[5] L. S. A. and Jabeena, T. Jayabarathi, and R. Aggarwal, "Review on optimization of wireless optical communication system," *Trends Opto-Electro Opt. Commun.*, vol. 4, pp. 9–19, Apr. 2019.

[6] R. K. J. A. Gupta, P. Anand, R. Khajuria, and S. Bhagat, "A survey of free space optical communication network channel over optical fiber cable communication," *Int. J. Comput. Appl.*, vol. 105, pp. 32–36, Jan. 2014.

[7] S. A. Al-Gailani, A. B. Mohammad, and R. Q. Shaddad, "Enhancement of free space optical link in heavy rain attenuation using multiple beam concept," *Optik*, vol. 124, no. 21, pp. 4798–4801, Nov. 2013, doi: 10.1016/j.ijleo.2013.01.098.

[8] S. A. Al-Gailani, A. B. Mohammad, R. Q. Shaddad, U. U. Sheikh, and M. A. Elmagzoub, "Hybrid WDM/multibeam free-space optics for multigigabit access network," *Photonic Netw. Commun.*, vol. 29, no. 2, pp. 138–145, Apr. 2015, doi: 10.1007/s11107-014-0482-y.

[9] J. A. R. P. de Carvalho, H. Veiga, P. A. J. Gomes, C. F. F. P. R. Pacheco, and A. D. Reis, "Experimental performance study of a very high speed free space optics link at the university of beira interior campus: A case study," in *Proc. IEEE Int. Symp. Signal Process. Inf. Technol.*, Dec. 2008, pp. 154–157, doi: 10.1109/ISSPIT.2008.4775657.

[10] O. Bouchet and P.-N. Favennec, *Wireless Optical Communication Title*. Hoboken, NJ, USA: Wiley, 2012.

[11] A. S. Hamza, J. S. Deogun, and D. R. Alexander, "Classification framework for free space optical communication links and systems," *IEEE Commun. Surveys Tuts.*, vol. 21, no. 2, pp. 1346–1382, 2nd Quart., 2019, doi: 10.1109/COMST.2018.2876805.

[12] N. Badar and R. K. Jha, "Performance comparison of various modulation schemes over free space optical (FSO) link employing Gamma–Gamma fading model," *Opt. Quantum Electron.*, vol. 49, no. 5, p. 192, May 2017.

[13] J. Pourahmadazar, S. Sahebghalam, S. Abazari Aghdam, and M. Nouri, "A millimeter-wave fresnel zone plate lens design using perforated 3D printing material," in *IEEE MTT-S Int. Microw. Symp. Dig.*, Jul. 2018, pp. 1–3.

[14] D. C. Calvo, A. L. Thangawng, M. Nicholas, and C. N. Layman, "Thin fresnel zone plate lenses for focusing underwater sound," *Appl. Phys. Lett.*, vol. 107, no. 1, Jul. 2015, Art. no. 014103.

[15] A. G. Alkholidi and K. S. Altowij, "Free space optical communications—Theory and practices," *Contemp. Issues Wireless Commun.*, vol. 159, p. 212, Nov. 2014, doi: 10.5772/58884.

[16] J. Mikoáajczyk, Z. Bielecki, M. Bugajski, J. Piotrowski, J. Wojtas, W. Gawron, D. Szabra, and A. Prokopiuk, "Analysis of free-space optics development," *Metrol. Meas. Syst.*, vol. 24, no. 4, pp. 653–674, Dec. 2017.

[17] J. Singh and N. Kumar, "Performance analysis of different modulation format on free space optical communication system," *Optik*, vol. 124, no. 20, pp. 4651–4654, Oct. 2013, doi: 10.1016/j.ijleo.2013.02.014.

[18] F. A. Wahab, T. K. Leong, H. Zulkifli, M. I. Ibrahim, M. A. B. Talib, N. A. Zamri, and O. K. Ibrahim, "Multiple transmitters & receivers for free space optical communication link performance analysis," *J. Telecommun. Electron. Comput. Eng.*, vol. 8, no. 5, pp. 29–32, 2016.

[19] M. C. Teich and B. Saleh, *Fundamentals of Photonics*, vol. 3. Hoboken, NJ, USA: Wiley, 1991.

[20] A. Malik and P. Singh, "Free space optics: Current applications and future challenges," *Int. J. Opt.*, vol. 2015, pp. 1–7, 2015, doi: 10.1155/2015/945483.

[21] S. Saurabh, "To study the effect of fog, snow and rain attenuation on FSO link," *CT Int. J. Inf. Commun. Technol.*, vol. 2, no. 1, pp. 16–22, 2014.

[22] S. R. Forrest, "Optical detectors: Three contenders: Depending on the application, the photoeonductor, p-i-n diode, or avalanche photodiode may prove the best choice," *IEEE Spectr.*, vol. 23, no. 5, pp. 76–84, May 1986, doi: 10.1109/mspec.1986.6370907.

[23] J. C. Juarez, A. Dwivedi, A. R. Hammons, S. D. Jones, V. Weerackody, and R. A. Nichols, "Free-space optical communications for next-generation military networks," *IEEE Commun. Mag.*, vol. 44, no. 11, pp. 46–51, Nov. 2006, doi: 10.1109/MCOM.2006.248164.

[24] S. Trisno, "Design and analysis of advanced free space optical communication systems," Ph.D. dissertation, Univ. Maryland, College Park, MD, USA, 2006.

[25] S. A. Al-Gailani, A. B. Mohammad, R. Q. Shaddad, and M. Y. Jamaludin, "Single and multiple transceiver simulation modules for free-space optical channel in tropical malaysian weather," in *Proc. IEEE Bus. Eng. Ind. Appl. Colloq. (BEIAC)*, Apr. 2013, pp. 613–616, doi: 10.1109/BEIAC.2013.6560203.

[26] I. I. Kim, M. Mitchell, and E. J. Korevaar, "Measurement of scintillation for free-space laser communication at 785 nm and 1550 nm," *Proc. SPIE Opt. Wireless Commun.*, vol. 3850, pp. 49–62, Dec. 1999.

[27] F. D. Kashani, M. Reza Hedayati rad, M. Reza Mahzoun, and B. Ghafary, "Beam propagation analysis of a multi beam FSO system with partially flat-topped laser beams in turbulent atmosphere," *Optik*, vol. 123, no. 10, pp. 879–886, May 2012, doi: 10.1016/j.ijleo.2011.05.036.

[28] N. H. Md Noor, W. Al-Khateeb, and A. W. Naji, "Experimental evaluation of multiple transmitters/receivers on free space optics link," *Proc. IEEE Student Conf. Res. Dev.*, Dec. 2011, vol. 2, pp. 128–133, doi: 10.1109/SCOReD.2011.6148721.

[29] N. H. Md Noor, A. W. Naji, and W. Al-Khateeb, "Performance analysis of a free space optics link with multiple transmitters/receivers," *IIUM Eng. J.*, vol. 13, no. 1, pp. 49–58, Apr. 2012, doi: 10.31436/iiumej.v13i1.271.
[30] B. Willebrand, H. and Ghuman, *Free Space Optics: Enabling Optical Connectivity in Today's Networks*. Indianapolis, IN, USA: SAMS, 2002.
[31] A. Elzanaty and M.-S. Alouini, "Adaptive coded modulation for IM/DD free-space optical backhauling: A probabilistic shaping approach," 2020, *arXiv:2005.02129*. [Online]. Available: http://arxiv.org/abs/2005.02129
[32] L. Gao, C. Gao, T. Zhu, Y. Li, Y. Long Cao, and G. Yin, "Incoherent optical modulation of graphene based on inline fiber Mach-Zehnder interferometer," *Opt. InfoBase Conf. Pap.*, vol. 122, pp. 5–6, Dec. 2017, doi: 10.1364/ol.42.001708.
[33] H. Sarangal, A. Singh, J. Malhotra, and S. Chaudhary, "A cost effective 100 GBPS hybrid MDM–OCDMA–FSO transmission system under atmospheric turbulences," *Opt. Quantum Electron.*, vol. 49, no. 5, pp. 1–10, May 2017, doi: 10.1007/s11082-017-1019-2.
[34] K. Kiasaleh, "Performance of APD-based, PPM free-space optical communication systems in atmospheric turbulence," *IEEE Trans. Commun.*, vol. 53, no. 9, pp. 1455–1461, Sep. 2005.
[35] H. Liu, R. Liao, Z. Wei, Z. Hou, and Y. Qiao, "BER analysis of a hybrid modulation scheme based on PPM and MSK subcarrier intensity modulation," *IEEE Photon. J.*, vol. 7, no. 4, pp. 1–10, Aug. 2015, doi: 10.1109/JPHOT.2015.2449265.
[36] Z. Wang, W.-X. Shi, and P.-X. Wu, "PDM-DPSK-MPPM hybrid modulation for multi-hop free-space optical communication," *Optoelectronics Lett.*, vol. 12, no. 6, pp. 450–454, Nov. 2016, doi: 10.1007/s11801-016-6192-1.
[37] G. Kaur, H. Singh, and A. Singh Sappal, "Free space optical using different modulation techniques – a review," *Int. J. Eng. Trends Technol.*, vol. 43, no. 2, pp. 109–115, Jan. 2017, doi: 10.14445/22315381/ijett-v43p218.
[38] G. Z. Popoola, *Optical Wireless Communications: System and Channel Modelling With MATLAB*. New York, NY, USA: CRC Press, 2013.
[39] J. Lesh, "Capacity limit of the noiseless, energy-efficient optical PPM channel," *IEEE Trans. Commun.*, vol. 31, no. 4, pp. 546–548, Apr. 1983.
[40] B. Moision and J. Hamkins, "Multipulse PPM on discrete memoryless-Channels," *Jet Propuls. Lab*, vol. 4, pp. 142–160, Dec. 2005.
[41] Y. Fan and G. Rj, "Comparison of pulse position modulation and pulse width modulation for application in optical communications," *Opt. Eng.*, vol. 46, no. 6, pp. 65–72, 2007.
[42] Z. Ghassemlooy, A. R. Hayes, N. L. Seed, and E. D. Kaluarachchi, "Digital pulse interval modulation for optical communications," *IEEE Commun. Mag.*, vol. 36, no. 12, pp. 95–99, 1998.
[43] M. A. A. Ali, "Performance analysis of terrestrial WDM-FSO link under different weather channel," *World Sci. News*, vol. 56, pp. 33–44, Oct. 2016.
[44] N. Avlonitis, E. M. Yeatman, M. Jones, and A. Hadjifotiou, "Multilevel amplitude shift keying in dispersion uncompensated optical systems," *IEE Process. Optoelectron.*, vol. 153, no. 3, pp. 101–108, Jun. 2006.
[45] S. Hranilovic, *Wireless Optical Communication Systems*. New York, NY, USA: Springer-Verlag, 2005.
[46] T. YoussefElganimi, "Performance comparison between OOK, PPM and PAM modulation schemes for free space optical (FSO) communication systems: Analytical study," *Int. J. Comput. Appl.*, vol. 79, no. 11, pp. 22–27, Oct. 2013, doi: 10.5120/13786-1838.
[47] Z. Wang, W. D. Zhong, S. Fu, and C. Lin, "Performance comparison of different modulation formats over free-space optical (FSO) turbulence links with space diversity reception technique," *IEEE Photonic J.*, vol. 1, no. 6, pp. 32–40, Dec. 2009.
[48] Y. Han and G. Li, "Theoretical sensitivity of direct-detection multilevel modulation formats for high spectral efficiency optical communications," *IEEE J. Sel. Topics Quantum Electron.*, vol. 12, no. 4, pp. 571–580, Jul. 2006.
[49] D. Hossen and G. S. Alim, "Performane evaluation of the free space optical (FSO) communication with the effects of the atmospheric turbulances," BRAC Univ., Dhaka, Bangladesh, Tech. Rep., Jan. 2008.
[50] J. M. Hamamreh, H. M. Furqan, and H. Arslan, "Classifications and applications of physical layer security techniques for confidentiality: A comprehensive survey," *IEEE Commun. Surveys Tuts.*, vol. 21, no. 2, pp. 1773–1828, 2nd Quart., 2019, doi: 10.1109/COMST.2018.2878035.
[51] I. K. Son and S. Mao, "A survey of free space optical networks," *Digit. Commun. Netw.*, vol. 3, no. 2, pp. 67–77, May 2017.
[52] (2008). *Malaysian Meteorological Department Website*. [Online]. Available: http://www.met.gov.my
[53] N. Karafolas, "11 Optical satellite networking: The concept of a global satellite optical transport network," *Near-Earth Laser Commun.*, vol. 1, p. 141, Dec. 2018.
[54] V. W. S. Chan, "Optical satellite networks," *J. Lightw. Technol.*, vol. 21, no. 11, p. 2811, 2003.
[55] C. C. Davis, I. I. Smolyaninov, and S. D. Milner, "Flexible optical wireless links and networks," *IEEE Commun. Mag.*, vol. 41, no. 3, pp. 51–57, Mar. 2003.
[56] Rashmeet, A. Gupta, and R. Goyal, "Channel performance evaluation of wireless communication networks," in *Proc. 5th Int. Conf. Parallel, Distrib. Grid Comput. (PDGC)*, Dec. 2018, pp. 165–170.
[57] D. Giggenbach, J. Horwath, and B. Epple, "Optical satellite downlinks to optical ground stations and high-altitude platforms," in *Proc. 16th IST Mobile Wireless Commun. Summit*, Jul. 2007, pp. 331–349.
[58] A. Al-Kinani, C.-X. Wang, L. Zhou, and W. Zhang, "Optical wireless communication channel measurements and models," *IEEE Commun. Surveys Tuts.*, vol. 20, no. 3, pp. 1939–1962, 3rd Quart., 2018.
[59] I. K. Son and S. Mao, "Optical networks, digital communications and networks," Tech. Rep., 2016.
[60] D.-R. Kim, S.-H. Yang, H.-S. Kim, Y.-H. Son, and S.-K. Han, "Outdoor visible light communication for inter- vehicle communication using controller area network," in *Proc. 4th Int. Conf. Commun. Electron. (ICCE)*, Aug. 2012, pp. 31–34.
[61] S. Bloom, E. Korevaar, J. Schuster, and H. Willebrand, "Understanding the performance of free-space optics [invited]," *J. Opt. Netw.*, vol. 2, no. 6, pp. 178–200, Jun. 2003.
[62] K. V. Kiran, V. Kumar, A. K. Turuk, and S. K. Das, "Estimation of link margin for performance analysis of FSO network," *Commun. Comput. Inf. Sci.*, vol. 827, pp. 444–458, Dec. 2018, doi: 10.1007/978-981-10-8657-1_34.
[63] I. D. A. Singapore, "A trial-based study of FreeSpace optics systems in Singapore," Info Commun. Develop. Authority Singapore (iDA), Singapore, Tech. Rep., 2002.
[64] M. Uysal, C. Capsoni, A. B. Z. Ghassemlooy, and E. Udvary, *Optical Wireless Communications: An Emerging Technology*. Cham, Switzerland: Springer, 2016.
[65] P. V. and J. Vijay, "Comparative analysis of free space optics and single mode fiber," *Int. J. Adv. Eng. Manag. Sci.*, vol. 2, no. 1, 2016, Art. no. 239367.
[66] M. S. Alam, S. A. Shawkat, G. Kitazumi, and M. Matsumoto, "IrBurst modeling and performance evaluation for large data block exchange over high-speed IrDA links," *IEICE Trans. Commun.*, vols. E91–B, no. 1, pp. 274–285, Jan. 2008, doi: 10.1093/ietcom/e91-b.1.274.
[67] P. S. Ray, "Broadband complex refractive indices of ice and water," *Appl. Opt.*, vol. 11, no. 8, pp. 1836–1844, Aug. 1972.
[68] H. Willebrand and B. S. Ghuman, *Free Space Optics: Enabling Optical Connectivity in Today's Networks*. Indianapolis, IN, USA: SAMS, 2002.
[69] Y. Kaymak, R. Rojas-Cessa, J. Feng, N. Ansari, M. Zhou, and T. Zhang, "A survey on acquisition, tracking, and pointing mechanisms for mobile free-space optical communications," *IEEE Commun. Surveys Tuts.*, vol. 20, no. 2, pp. 1104–1123, 2nd Quart., 2018, doi: 10.1109/COMST.2018.2804323.
[70] X. Liu, "Free-space optics optimization models for building sway and atmospheric interference using variable wavelength," *IEEE Trans. Commun.*, vol. 57, no. 2, pp. 492–498, Feb. 2009, doi: 10.1109/TCOMM.2009.02.070089.
[71] A. Harris, J. J. Sluss, H. H. Refai, and P. G. LoPresti, "Alignment and tracking of a free-space optical communications link to a UAV," in *Proc. AIAA/IEEE Digit. Avion. Syst. Conf.*, 2005, vol. 1, pp. 1–9, doi: 10.1109/DASC.2005.1563300.
[72] J. Latal, J. Vitasek, L. Hajek, A. Vanderka, R. Martinek, and V. Vasinek, "Influence of simulated atmospheric effect combined with modulation formats on FSO systems," *Opt. Switching Netw.*, vol. 33, pp. 184–193, Jul. 2019, doi: 10.1016/j.osn.2018.01.001.
[73] S. Babani, Y. Abdulmalik, A. Abdul'aziz, A. Loko, and M. Gajibo, "Free space optical communication: The main challenges and its possible solution," *Int. J. Sci. Eng. Res.*, vol. 5, pp. 1–4, Jul. 2014.
[74] M. Achour, "Simulating atmospheric free-space optical propagation; Part II: Haze, fog, and low clouds attenuations," *Opt. Wireless Commun.*, vol. 4873, p. 1, Dec. 2002, doi: 10.1117/12.458571.
[75] U. Korai, L. Luini, and R. Nebuloni, "Model for the prediction of rain attenuation affecting free space optical links," *Electronics*, vol. 7, no. 12, p. 407, Dec. 2018, doi: 10.3390/electronics7120407.

[76] R. A. H. Mathew, Jr., *Cloud Dynamics*, vol. 104. New York, NY, USA: Academic, 2014.
[77] A. J. Townsend, "A study of the raindrop size distribution and its effect on microwave attenuation," Ph.D. dissertation, Dept. Electron. Elect. Eng., Univ. Bath, Bath, U.K., 2011.
[78] R. Houze, "Stratiform precipitation in regions of convection," *Bull. Amer. Meteor. Soc*, vol. 78, pp. 2179–2195, Dec. 1997.
[79] R. K. Crane, "Space-time structure of rain rate fields," *J. Geophys. Res.*, vol. 95, no. D3, pp. 2011–2020, 1990, doi: 10.1029/JD095iD03p02011.
[80] T. G. Konrad, "Statistical Models of Summer Rainshowers Derived From Fine-Scale Radar Observations.," *J. Appl. Meteorol.*, vol. 17, no. 2, pp. 171–188, 1978, doi: 10.1175/1520-0450(1978)017<0171:SMOSRD>2.0.CO.2.
[81] J. Goldhirsh, "Two-dimension visualization of rain cell structures," *Radio Sci.*, vol. 35, no. 3, pp. 713–729, May 2000.
[82] M. K. Yau and R. R. Rogers, "An inversion problem on inferring the size distribution of precipitation areas from raingage measurements," *J. Atmos. Sci.*, vol. 41, no. 3, pp. 439–448, Feb. 1984.
[83] L. Feral, F. Mesnard, H. Sauvageot, L. Castanets, and J. Lemorton, "Rain cells shape and orientation distribution in South-West of France," *Phys. Chem. Earth B, Hydrol. Ocean. Atmos.*, vol. 25, nos. 10–12, pp. 1073–1078, 2000, doi: 10.1016/S1464-1909(00)00155-6.
[84] *Characteristics of Precipitation for Propagation Modelling*, document ITU-R. 2012:837-6, 2012.
[85] R. P. Series, *Propagation Data and Prediction Methods Required for the Design of Terrestrial Line-of-Sight Systems*, document Rec. ITU-R P.530-12, ITU, Geneva, Switzerland, 2006, pp. 1–47.
[86] S. A. Zabidi, M. R. Islam, W. A. Khateeb, and A. W. Naji, "Investigating of rain attenuation impact on free space optics propagation in tropical region," in *Proc. 4th Int. Conf. Mechatronics (ICOM)*, May 2011, pp. 17–19, doi: 10.1109/ICOM.2011.5937121.
[87] M. Thurai, V. Bringi, P. N. Gatlin, W. A. Petersen, and M. T. Wingo, "Measurements and modeling of the full rain drop size distribution," *Atmosphere*, vol. 10, no. 1, pp. 1–16, 2019, doi: 10.3390/atmos10010039.
[88] F. Giannetti, R. Reggiannini, M. Moretti, E. Adirosi, L. Baldini, L. Facheris, A. Antonini, S. Melani, G. Bacci, A. Petrolino, and A. Vaccaro, "Real-time rain rate evaluation via satellite downlink signal attenuation measurement," *Sensors*, vol. 17, no. 8, p. 1864, Aug. 2017, doi: 10.3390/s17081864.
[89] J. Testud, S. Oury, R. A. Black, P. Amayenc, and X. Dou, "The concept of 'normalized' distribution to describe raindrop spectra: A tool for cloud physics and cloud remote sensing," *J. Appl. Meteorol.*, vol. 40, no. 6, pp. 1118–1140, 2001, doi: 10.1175/1520-0450(2001)040<1118:TCONDT>2.0.CO.2.
[90] A. C. Best, "The size distribution of raindrops," *Quart. J. Roy. Meteorol. Soc.*, vol. 76, no. 327, pp. 16–36, Jan. 1950, doi: 10.1002/qj.49707632704.
[91] G. Feingold and Z. Levin, "The lognormal fit to raindrop spectra from frontal convective clouds in Israel.," *J. Climate Appl. Meteorol.*, vol. 25, no. 10, pp. 1346–1363, 1986, doi: 10.1175/1520-0450(1986)025<1346:TLFTRS>2.0.CO.2.
[92] D. Atlas and C. W. Ulbrich, "Path and area-integrated rainfall measurement by microwave attenuation in the 1–3 cm band," *J. Appl. Meteorol. Climatol.*, vol. 16, pp. 406–413, Dec. 1977.
[93] J. Joss and E. G. Gori, "Shapes of raindrop size distributions," *J. Appl. Meteorol.*, vol. 17, no. 7, pp. 1054–1061, 1978, doi: 10.1175/1520-0450(1978)017<1054:sorsd>2.0.co.2.
[94] C. W. Ulbrich, "Natural variations in the analytical form of the raindrop size distribution," *J. Climate Appl. Meteorol.*, vol. 22, no. 10, pp. 1764–1775, 1983, doi: 10.1175/1520-0450(1983)022<1764:NVITAF>2.0.CO.2.
[95] G. Soni and J. Malhotra, "Free space optics system: Performance and link availability," *Ijccr*, vol. 1, no. 3, 2011.
[96] R. S. L. and de da Silva Mello and E. Costa, "Rain attenuation measurements at 15 and 18 GHz," *Electron. Lett.*, vol. 38, pp. 197–198, Dec. 2002.
[97] H. Alma and W. Al-Khateeb, "Effect of weather conditions on quality of free space optics links (with focus on Malaysia)," in *Proc. Int. Conf. Comput. Commun. Eng.*, May 2008, pp. 1206–1210, doi: 10.1109/ICCCE.2008.4580797.
[98] C.-S. Lu, Z.-W. Zhao, Z.-S. Wu, L.-K. Lin, P. Thiennviboon, X. Zhang, and Z.-F. Lv, "A new rain attenuation prediction model for the Earth-space links," *IEEE Trans. Antennas Propag.*, vol. 66, no. 10, pp. 5432–5442, Oct. 2018, doi: 10.1109/TAP.2018.2854181.
[99] L. D. Emiliani, L. Luini, and C. Capsoni, "Extension of ITU-R method for conversion of rain rate statistics from various integration times to one minute," *Electron. Lett.*, vol. 44, no. 8, pp. 557–558, Apr. 2008.
[100] A. Z. Suriza, I. Md Rafiqul, A. K. Wajdi, and A. W. Naji, "Proposed parameters of specific rain attenuation prediction for free space optics link operating in tropical region," *J. Atmos. Solar-Terrestrial Phys.*, vol. 94, pp. 93–99, Mar. 2013, doi: 10.1016/j.jastp.2012.11.008.
[101] J. S. Ojo, M. O. Ajewole, and S. K. Sarkar, "Rain rate and rain attenuation prediction for satellite communication in ku and Ka bands over Nigeria," *Prog. Electromagn. Res. B*, vol. 5, pp. 207–223, 2008, doi: 10.2528/pierb08021201.
[102] R. K. Crane and A. W. Dissanayake, "Acts propagation experiment: Attenuation distribution observations and prediction model comparisons," *Proc. IEEE*, vol. 85, no. 6, pp. 879–891, Jun. 1997, doi: 10.1109/5.598411.
[103] C. I. Kourogiorgas, A. D. Panagopoulos, and J. D. Kanellopoulos, "On the Earth-space site diversity modeling: A novel physical-mathematical outage prediction model," *IEEE Trans. Antennas Propag.*, vol. 60, no. 9, pp. 4391–4397, Sep. 2012, doi: 10.1109/TAP.2012.2207073.
[104] W. Zhang and N. Moayeri. (1999). *Power-Law Parameters of Rain Specific Attenuation*. [Online]. Available: http://scholar.google.com/scholar?hl=en&btnG=Search&q=intitle:Power-Law+Parameters+of+Rain+Specific+Attenuation#0
[105] S. A. Zabidi, M. R. Islam, W. Al-Khateeb, and A. W. Naji, "Analysis of rain effects on terrestrial free space optics based on data measured in tropical climate," *IIUM Eng. J.*, vol. 12, no. 5, pp. 45–51, Jan. 2012, doi: 10.31436/iiumej.v12i5.232.
[106] *Specific Attenuation Model for Rain for Use in Prediction Methods*, 1999.
[107] *Prediction Methods Required for The Design of Terrestrial Free-Space Optical Links*, document ITU-Recommendation 1814, 2007. [Online]. Available: https://www.itu.int/dms_pubrec/itu-r/rec/p/R-REC-P.1814-0-200708-I!!PDF-E.pdf
[108] T. H. Carbonneau and D. R. Wisely, "Opportunities and challenges for optical wireless: The competitive advantage of free space telecommunications links in today's crowded marketplace," in *Proc. Wireless Technol. Syst., Millimeter-Wave Opt.*, Jan. 1998, pp. 119–128.
[109] M. A. Awang and J. Din, "Comparison of the rain drop size distribution model in tropical region," in *Proc. RF Microw. Conf.*, 1992, pp. 20–22, doi: 10.1109/rfm.2004.1411063.
[110] N. Aida M. Nor, M. R. Islam, and W. Al-Khateeb, "Atmospheric effects on free space Earth-to-Satellite optical link in tropical climate," *Int. J. Comput. Sci., Eng. Appl.*, vol. 3, no. 1, pp. 17–36, Feb. 2013, doi: 10.5121/ijcsea.2013.3102.
[111] (2008). *Haze Watch Website*. [Online]. Available: http//www.hazeonline.or.id
[112] P. H. and J. Souza, "Free space optical communication systems: A feasibility study for deployment in Brazil," *J. Microw. Optoelectron.*, vol. 3, p. 58, May 2004.
[113] Z. Rahman, S. M. Zafaruddin, and V. K. Chaubey, "Performance of opportunistic receiver beam selection in multiaperture OWC systems over foggy channels," *IEEE Syst. J.*, vol. 14, no. 3, pp. 4036–4046, Sep. 2020.
[114] M. S. Khan, "Further results on fog modeling for terrestrial free-space optical links," *Opt. Eng.*, vol. 51, no. 3, Apr. 2012, Art. no. 031207.
[115] A. Alatrash and E. Matida, "Characterization of medication velocity and size distribution from pressurized metered-dose inhalers by phase Doppler anemometry," *J. Aerosol Med. Pulmonary Drug Del.*, vol. 29, no. 6, pp. 501–513, Dec. 2016.
[116] M. Grabner and V. Kvicera, "Fog attenuation dependence on atmospheric visibility at two wavelengths for FSO link planning," in *Proc. Loughborough Antennas Propag. Conf.*, Nov. 2010, pp. 193–196.
[117] B. S. S. Naimullah, S. Hitam, N. S. M. Shah, M. Othman, S. B. A. Anas, and M. K. Abdullah, "Analysis of the effect of haze on free space optical communication in the malaysian environment," in *Proc. IEEE Int. Conf. Telecommun. Malaysia Int. Conf. Commun.*, 2007, pp. 391–394, doi: 10.1109/ICTMICC.2007.4448669.
[118] I. I. Kim, B. McArthur, and E. J. Korevaar, "Comparison of laser beam propagation at 785 nm and 1550 nm in fog and haze for optical wireless communications," *Opt. Wireless Commun.*, vol. 4214, pp. 26–37, Feb. 2001, doi: 10.1117/12.417512.
[119] P. W. Kruse, L. D. McGlauchlin, and R. B. McQuistan, *Elements of Infrared Technology: Generation, Transmission and Detection*, vol. 1. New York, NY, USA: Wiley, 1962.
[120] R. M. Pierce, J. Ramaprasad, and E. C. Eisenberg, "Optical attenuation in fog and clouds," in *Proc. Opt. Wireless Commun.*, Nov. 2001, pp. 58–71.

[121] *Propagation data required for the design of terrestrial free-space optical links ITU-R Recommendation*, document ITU-R P.1817, 2012.
[122] O. M. Hasan and M. A. Taha, "Optimized FSO system performance over atmospheric turbulence channels with pointing error and weather conditions," *Radioengineering*, vol. 25, no. 4, pp. 658–665, Sep. 2016, doi: 10.13164/re.2016.0658.
[123] M. A. Al-Habash, "Mathematical model for the irradiance probability density function of a laser beam propagating through turbulent media," *Opt. Eng.*, vol. 40, no. 8, p. 1554, Aug. 2001, doi: 10.1117/1.1386641.
[124] M. S. Awan, P. Brandl, E. Leitgeb, F. Nadeem, L. Csugai-Horvath, and R. Nebuloni, "Transmission of high data rate optical signals in fog and snow conditions," in *Proc. 1st Int. Conf. Wireless Commun., Veh. Technol., Inf. Theory Aerosp. Electron. Syst. Technol.*, May 2009, pp. 702–706, doi: 10.1109/WIRELESSVITAE.2009.5172534.
[125] X. Wu, P. Liu, and M. Matsumoto, "A study on atmospheric turbulence effects in full-optical free-space communication systems," in *Proc. Int. Conf. Comput. Intell. Softw. Eng.*, Sep. 2010, pp. 1–5, doi: 10.1109/WICOM.2010.5600908.
[126] P. Kumar, P. Verma, R. Singh, and R. K. Patel, *Proceeding of International Conference on Intelligent Communication, Control and Devices*. Cham, Switzerland: Springer, 2018, pp. 979–989, 2016, doi: 10.1007/978-981-10-1708-7.
[127] E. E. Elsayed, B. B. Yousif, and M. M. Alzalabani, *Performance Enhancement of the Power Penalty in DWDM FSO Communication Using DPPM and OOK Modulation*, vol. 50, no. 7. Cham, Switzerland: Springer, 2018.
[128] A. B. Mohammad, "Optimization of FSO system in tropical weather using multiple beams," in *Proc. IEEE 5th Int. Conf. Photon. (ICP)*, Sep. 2014, pp. 109–112, doi: 10.1109/ICP.2014.7002326.
[129] H. A. Fadhil, A. Amphawan, H. A. B. Shamsuddin, T. Hussein Abd, H. M. R. Al-Khafaji, S. A. Aljunid, and N. Ahmed, "Optimization of free space optics parameters: An optimum solution for bad weather conditions," *Optik*, vol. 124, no. 19, pp. 3969–3973, Oct. 2013, doi: 10.1016/j.ijleo.2012.11.059.
[130] Hitam, "Performance analysis on 16-channels wavelength division multiplexing in free space optical transmission under tropical regions environment," *J. Comput. Sci.*, vol. 8, no. 1, pp. 145–148, Jan. 2012.
[131] M. S. Ab-Rahman, H. Guna, M. H. Harun, S. D. Zan, and K. Jumari, "Cost-effective fabrication of self-made 1 12 polymer optical fiber-based optical splitters for automotive application," *Am. J. Eng. Appl. Sci.*, vol. 2, p. 252, Dec. 2009.
[132] M. Grover, P. Singh, P. Kaur, and C. Madhu, "Multibeam WDM-FSO system: An optimum solution for clear and hazy weather conditions," *Wireless Pers. Commun.*, vol. 97, no. 4, pp. 5783–5795, Dec. 2017, doi: 10.1007/s11277-017-4810-2.
[133] F. M. Mirabella, *Modern Techniques in Applied Molecular Spectroscopy* vol. 14. Hoboken, NJ, USA: Wiley, 1998.
[134] M. Ijaz, Z. Ghassemlooy, A. Gholami, and X. Tang, "Smoke attenuation in free space optical communication under laboratory controlled conditions," in *Proc. 7'th Int. Symp. Telecommun. (IST)*, Sep. 2014, pp. 758–762.

SAMIR AHMED AL-GAILANI (Member, IEEE) started his career as a Senior Lecturer with the Higher Technical Institute for applied B.Sc. degree in Aden, Yemen, in 1992. He received the Ph.D. degree in the field of optoelectronics from Universiti Technologi Malaysia (UTM), in 2014, with the Best Student Award. Since then, he has been given various responsibilities, including teaching, a Postdoctoral Fellow, supervising laboratory sessions, supervising post-graduate students and undergraduate students, an Academic Advisor, the Head of the Laboratory, the Head of the Research Group, the Chairman, and a member of different committees, conducting short courses and training. He has authored 20 ISI papers and has an H-index of 7 and total citations of 212, and presented more than 90 papers in reputed refereed conferences. He also successfully supervised nine postgraduate students.

MOHD FADZLI MOHD SALLEH (Member, IEEE) was born in Bagan Serai, Malaysia. He received the B.S. degree in electrical engineering from Polytechnic University, Brooklyn, NY, USA, in 1995, the M.S. degree in communication engineering from the University of Manchester Institute of Science and Technology, Manchester, U.K., in 2002, and the Ph.D. degree from the University of Strathclyde, Glasgow, U.K., in 2006. He was a Software Engineer with the Research and Development Department, Motorola Penang, until July 2001. He is currently an Associate Professor with the School of Electrical and Electronic Engineering, Universiti Sains Malaysia, Nibong Tebal, Malaysia. He has supervised 12 Ph.D. degree students to graduation. His research interests include source coding and signal processing for application in telecommunications, and wireless communication networks.

ALI AHMED SALEM (Member, IEEE) received the M.Eng. degree in electrical power engineering from University Tun Hussein Onn Malaysia (UTHM), in 2016, where he is currently pursuing the Ph.D. degree in high voltage with the Faculty of Electrical Engineering. His research interest includes the dynamic arc modeling of pollution flashover on high-voltage outdoor insulators.

REDHWAN QASEM SHADDAD was born in Ibb, Yemen, in 1979. He received the B.S. degree (Hons.) in electronics communication engineering from Ibb University, in 2003, and the master's degree in electrical-communication engineering from Universiti Teknologi Malaysia (UTM), Malaysia, in 2010, where he is currently pursuing the Ph.D. degree in electrical engineering. He has been working as an Associate Professor with Taiz University, Yemen, since 2003. His research interests include single-mode optical fiber communication, hybrid optical and wireless communication systems, optical OFDM communication, passive optical networks, free space optics, and neural networks.

USMAN ULLAH SHEIKH (Member, IEEE) received the B.Eng. degree in electrical and mechatronics engineering, the M.Eng. degree in telecommunications engineering, and the Ph.D. degree in image processing and computer vision from Universiti Teknologi Malaysia, in 2003, 2005, and 2009, respectively. He is currently a Senior Lecturer with Universiti Teknologi Malaysia, working on image processing for intelligent surveillance systems. His research interests include computer vision and embedded systems design. He is a member of IET and has published works in many IEEE conferences.

NASIR AHMED ALGEELANI received the B.E. degree in electrical power system from the University of Aden, Aden, Yemen, in 1997, and the M.E. degree in electrical power system engineering and the Ph.D. degree in high voltage engineering from University Technology Malaysia, in 2009 and 2014, respectively, and the Ph.D. degree from the High Voltage Engineering Department, University Technology Malaysia, in 2016. He is currently a Senior Lecturer with the High Voltage Department, Industrial Technical Institute (ITI), Aden, for nearly 25 years. He was then appointed as an Assistant Professor, up to date, at Al-Madinah International University, Malaysia. He has published as authored or coauthored more than 30 articles in various technical journals and conference proceedings. His research interests include high-voltage instrumentation, partial discharge, detection and warning systems, and condition monitoring of high-power equipment.

TARIK A. ALMOHAMAD (Student Member, IEEE) received the B.Sc. degree in information engineering from the Department of Telecommunication Engineering, Ittihad Private University, Syria, in 2008, with two distinguished awards as top two performers, the M.Sc. degree in electronic systems design engineering from USM, where he graduated as the Top Best, and the Ph.D. degree in 2019. He worked as a Lab Demonstrator with Ittihad Private University, from 2008 to 2010, and later joined the wireless cooperative communication projects at Universiti Sains Malaysia (USM), Nibong Tebal, Malaysia, as a Research Assistant. He was a recipient of USM Fellowship. His Ph.D. work is in the field of wireless and mobile systems where he investigated the identification of signal parameters in wireless communication systems.